nature methods

Perspective

https://doi.org/10.1038/s41592-026-03003-2

Toward a unified framework for determining conformational ensembles of disordered proteins

Received: 30 March 2025

Accepted: 15 December 2025

Published online: 09 March 2026

Check for updates

Hamidreza Ghafouri[1], Pavel Kadeřávek[2,3], Ana M. Melo[4,5], Maria Cristina Aspromonte[1], Pau Bernadó[6], Juan Cortés[7], Zsuzsanna Dosztányi[8], Gábor Erdős[8], Michael Feig[9], Giacomo Janson[9], Kresten Lindorff-Larsen[10], Frans A. A. Mulder[11], Peter Nagy[12,13,14,15], Richard Pestell[14,15,16,17,18], Damiano Piovesan[1], Marco Schiavina[19], Benjamin Schuler[20,21], Nathalie Sibille[22], Giulio Tesei[10], Peter Tompa[18,23], Michele Vendruscolo[24], Jiri Vondrasek[25], Wim Vranken[26,27,28,29,30], Lukas Zidek[2,3], Silvio C. E. Tosatto[1] ✉ & Alexander Miguel Monzon[1] ✉

Disordered proteins play essential roles in myriad cellular processes, yet their structural characterization remains a major challenge due to their dynamic and heterogeneous nature. Here we present a community-driven initiative to address this problem by advocating a unified framework for determining conformational ensembles of disordered proteins. Our aim is to integrate state-of-the-art experimental techniques with advanced computational methods, including knowledge-based sampling, enhanced molecular dynamics and machine learning models. The modular framework comprises three interconnected components: experimental data acquisition, computational ensemble generation and validation. The systematic development of this framework will ensure the accurate and reproducible determination of conformational ensembles of disordered proteins. We highlight the open challenges necessary to achieve this goal, including force-field accuracy, efficient sampling, and environmental dependence, advocating for collaborative benchmarking and standardized protocols.

Intrinsically disordered proteins and regions (hereafter collectively termed IDPs) are prevalent in eukaryotic proteomes, making up an estimated one-third of the human proteome[1]. These proteins exist as conformational ensembles of rapidly interconverting conformations (Box 1)[2]. IDPs are implicated in a broad range of signaling and regulatory functions, such as signal transduction, gene expression, genome organization, cell-cycle control and the formation of biomolecular condensates[3]. Consequently, IDPs are central targets for biological and medical research. A defining feature of IDPs is the link between the features of their conformational ensembles and their biological functions[4–6]. Understanding this relationship requires a robust framework for generating and analyzing conformational ensembles by combining computational and experimental techniques. In this Perspective, we advocate a unified framework for generating, analyzing and validating conformational ensembles of IDPs. This framework, developed through extensive discussions initiated during a workshop held in Prague in May 2023 (https://ml4ngp.eu/workshop-prague/), is structured around three key modules: (1) experimental observations informative of conformational ensembles, (2) computational generation of conformational ensembles consistent with the experimental information and (3) validation and comparison of the resulting conformational ensembles. By integrating insights from different

A full list of affiliations appears at the end of the paper. ✉e-mail: silvio.tosatto@unipd.it; alexander.monzon@unipd.it

https://doi.org/10.1038/s41592-026-03003-2

BOX 1

Glossary of terms used within the scope of this paper

Term	Definition
IDPs and disordered protein regions	Full-length proteins or protein regions that lack a stable ordered three-dimensional structure under physiological conditions
Conformers	Structures able to interconvert without making or breaking covalent bonds
Conformational collection	A set of conformers
Statistical ensemble	A conformational collection endowed with statistical weights
Conformational state	A thermodynamic state of a protein described by a statistical ensemble
Forward model	A computational framework that predicts experimental observables based on protein structures

methodologies in structural and computational biology, our goal is to progress toward establishing standardized processes that support integrative studies of IDPs. This modular framework (Fig. 1) underscores the importance of interdisciplinary collaboration in addressing the complexities of IDPs. By standardizing methodologies and establishing consensus within the scientific community, this framework seeks to enhance our understanding of the functions of IDPs, advance methodological rigor and accelerate therapeutic discovery.

Experimental techniques for studying IDP structural ensembles

NMR spectroscopy

Nuclear magnetic resonance (NMR) spectroscopy is uniquely suited for studying IDPs in solution, offering atomic-level information. This technique can capture the dynamic and heterogeneous nature of IDPs by exploiting the sensitivity of nuclear magnetic moments to their local magnetic environment. This sensitivity enables precise, selective and minimally invasive atomic-resolution assessment of structure, dynamics and interactions of IDPs under near-physiological conditions[7], typically following isotope labeling. Because IDPs have shallow free-energy landscapes, NMR observables are time averages that represent the statistical ensemble. However, the lack of information on individual states can be viewed as a fundamental limitation. The ensemble-averaged NMR parameters do not enable the specific reconstruction of individual conformers of the ensemble. Instead, the NMR parameters can be compared to those derived by forward models from simulated structural ensembles and thus benchmark the latter. Also, there are cases when some states of IDPs can be distinguished (for example, the presence of *cis* peptide bonds, which give rise to sets of additional signals[8–10]), or when the NMR spectrum clearly carries a mark of their distribution (for example, dynamics of molten globules manifested by line broadening[11]). NMR can also unveil sparsely populated NMR-invisible structural states by exploiting the transfer of magnetization between these states and NMR-visible states, through techniques like saturation transfer difference NMR and relaxation dispersion NMR. By analyzing the transferred magnetization, these techniques provide structural and dynamic information about minor states populated during structural transitions upon binding[12]. Moreover, NMR methods of selective detection of certain states have been designed (for example, paramagnetic relaxation enhancement (PRE) discussed below).

Key NMR observables in IDP studies. Several NMR parameters can be directly correlated to conformational properties of disordered proteins. Chemical shifts reflect local electronic environments and provide insights into secondary-structure propensities (SSPs)[13–15]. Computational tools such as ShiftX[16], SPARTA+[17], PPM[18] and CamShift[19] include forward models to predict chemical shifts from conformational ensembles (Table 1).

J-couplings, particularly three-bond couplings, directly report on backbone torsion angles through the Karplus equation[20]. These measurements are limited by the accuracy of the corresponding forward models and the availability of measurable *J*-couplings for specific torsion angles. For example, φ angles can reliably be probed[21]. Furthermore, ψ angles often require complementary approaches such as cross-correlated relaxation[22,23].

Residual dipolar couplings (RDCs) provide highly sensitive insights into IDP conformational preferences by reporting on the average orientation of bond vectors across all coexisting structures in solution[24,25]. RDCs reveal local secondary-structure biases, having an opposite sign in alpha-helices and extended structures. However, their detailed structural interpretation requires calculating or fitting the alignment tensor, which is particularly challenging for IDPs. To avoid this calculation, forward models that use the laboratory reference frame have been proposed[26]. Various alignment media exist, yet careful selection is crucial to avoid unwanted interactions that could alter measurements. Another use of RDCs is for the cross-validation of conformational ensembles derived from other NMR and small-angle X-ray scattering (SAXS) data, ensuring consistency in structural interpretations[27].

Relaxation rates offer insights into IDP dynamics across timescales. Through IDP-specific model-free formalism, the analysis of several backbone ^{15}N relaxation experiments in multiple magnetic fields probes the local and segmental motional amplitudes and their associated correlation times[28,29]. These data are also valuable for benchmarking molecular dynamics simulations, in which ensemble reweighting may be required to match experimental relaxation rates[30].

PRE is particularly powerful for disordered proteins, revealing transient long-range contacts and compact conformations within heterogeneous ensembles. For instance, PRE measurements have revealed transiently folded states in different IDPs[31–33], complementing global techniques like SAXS in characterizing conformational distributions[34–36]. Paramagnetic relaxation interference methods further expand this analysis, identifying correlated or anticorrelated motions in transiently compacted regions[37].

Because IDPs are highly sensitive to their environments, in-cell NMR is particularly indicated to study their context-dependent behavior under native-like conditions, such as in bacterial and eukaryotic cells. These studies, while technically challenging due to low sensitivity and high background noise, highlight the potential of NMR to bridge in vitro and in vivo IDP investigations[38–41].

smFRET

Single-molecule Förster resonance energy transfer (smFRET) is a powerful tool for investigating the conformational dynamics and structural heterogeneity of IDPs. Förster resonance energy transfer (FRET), a non-radiative energy transfer from an excited donor fluorophore to an acceptor fluorophore, is highly sensitive to donor–acceptor distances, following an inverse sixth-power relationship. This makes smFRET a spectroscopic ruler capable of measuring intermolecular and intramolecular distances within a 2–10-nm range[42]. Unlike ensemble-averaging methods, smFRET provides a unique ability to resolve subpopulations, detect rare states and capture dynamic transitions of individual molecules, making it particularly suited for IDP studies[43,44].

smFRET applications to IDPs. smFRET has been instrumental in studying IDPs under diverse conditions. It has been used to elucidate the conformational ensembles of IDPs in dilute solution[43,45,46] and

https://doi.org/10.1038/s41592-026-03003-2

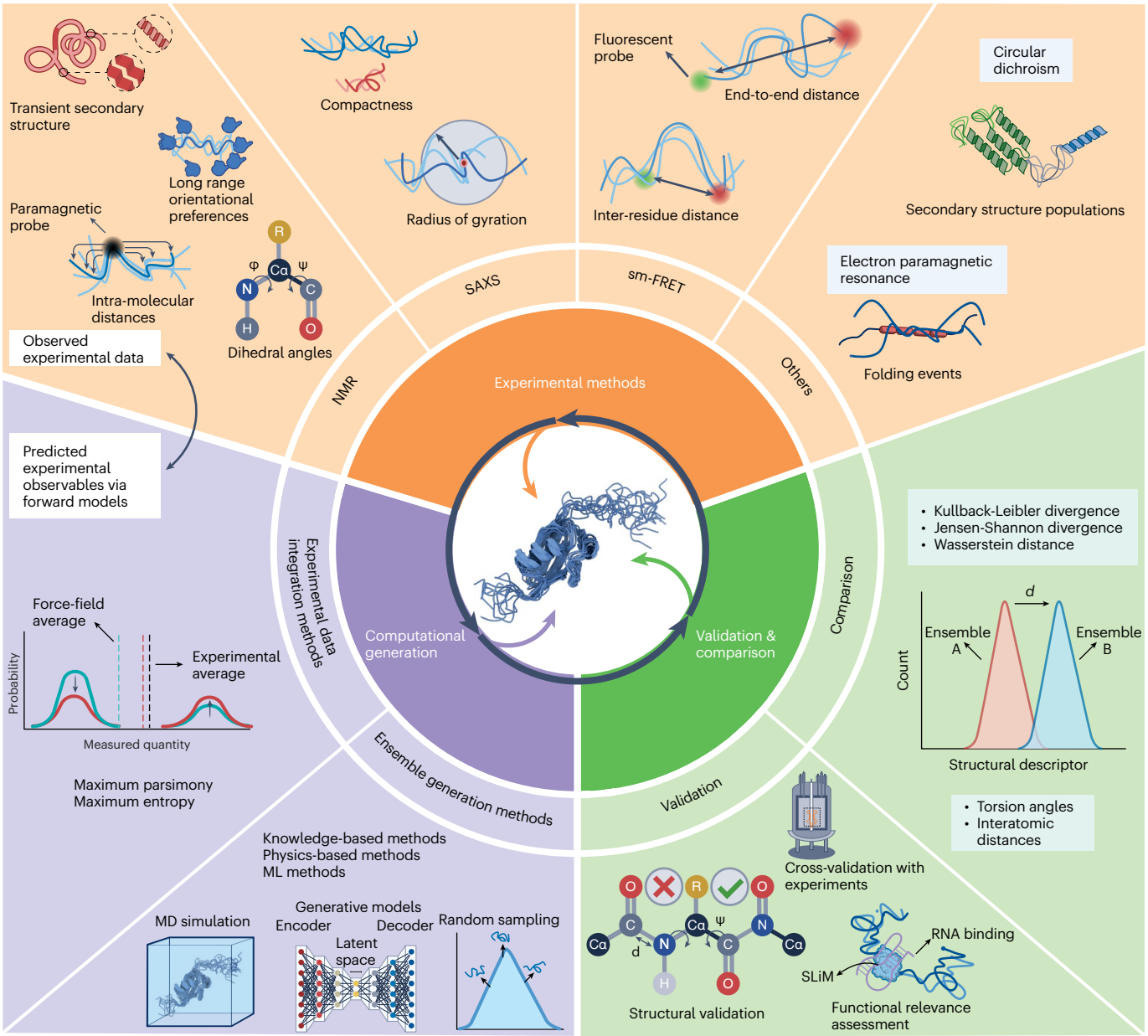

Fig. 1 | Schematic representation of the modular framework for the determination of conformational ensembles of IDPs. The illustration presents the modular framework for determining conformational ensembles of IDPs, comprising three interconnected modules: experimental methods, computational ensemble generation and validation and comparison. The first module focuses on experimental techniques such as NMR spectroscopy, single-molecule FRET, SAXS, circular dichroism and electron paramagnetic resonance spectroscopy. These methods provide local and global structural information for characterizing the heterogeneous and dynamic nature of IDPs. The second module of the framework addresses the computational determination of conformational ensembles of IDPs. This module involves the generation of conformational ensembles and the integration of experimental data obtained in the first module. Ensemble generation methods can be categorized into physics-based (molecular dynamics simulations), knowledge-based and machine learning methods. In addition, maximum parsimony and maximum entropy are the main approaches for the integration of experimental data. The role of forward models is crucial in this step since they link the experimental observables to the generated models to ensure the goodness of fit to observed experimental data. Lastly, the validation and comparison tools complete the circular process of determining IDP conformational ensembles. Validation can be achieved through compliance of structures in the ensemble with basic physicochemical rules (structural validation), cross-validation using complementary experimental data and functional relevance assessment. Comparison tools particularly involve statistical methods for analyzing distributions, such as Kullback–Leibler, Jensen–Shannon divergence scores and Wasserstein distances. MD, molecular dynamics; ML, machine learning. Figure created in BioRender; Ghafouri, H. https://biorender.com/aq5pa86 (2025).

crowded environments[47], including phase-separated biomolecular condensates[48,49] and live cells[50]. Furthermore, this technique has shed light on dynamic IDP complexes, revealing the interplay of transient structural states during functional interactions[44]. Single-molecule studies can be performed down to picomolar concentrations[42], avoiding the complications of aggregation and allowing functional/dysfunctional states of aggregation-prone IDPs to be probed[51–53].

smFRET experimental setup and protein labeling. smFRET experiments typically use either total internal reflection fluorescence

https://doi.org/10.1038/s41592-026-03003-2

Table 1 | Main experimental methods to determine structural ensembles of IDPs

Technique	Experimental measurement	Forward models/ computational tools/ theoretical models	Information content	Structural interpretation (for example, residue level versus global)	System perturbation	Environment (in vivo/in vitro/ in cell)	Reference database
NMR	Chemical shifts (traditional, ^{13}C-NMR, ...)	ShiftX, SHIFTS, Sparta, PPM1, CamShift	Local SSP; ensemble-averaged deviations from random coil values. Limited	Dihedral angles, secondary structure population, dynamics	Isotope labeling	In cell/in vitro	https://bmrb.io/
		SSP, RCI, d2D, Shiftcrypt					
	PRE, paramagnetic relaxation interference	Dipole-dipole equation + correlation function, DEER-PREdict, MMM (Multiscale Modeling of Macromolecules)	Ensemble-averaged distances between spin labels and nuclei; provides insight into transient, weak or low-population interactions and structural heterogeneity.	Distances/regions with correlated folding/dynamics	Chemical attachment of a paramagnetic label		
		Covariance/ correlation analysis					
	Relaxation rates	Model to data: molecular dynamics simulation + correlation function analysis + weighting	Time constants for intramolecular and global motions; order parameters reflecting flexibility; reveals timescales of molecular motions.	Correlation times + weights/order parameters	Isotope labeling		
		Data to model: spectral density mapping, model-free analysis, IMPACT					
	DOSY	Data to model: Stokes–Einstein equation	Global hydrodynamic radius; informs on chain expansion or compaction	Translation diffusion coefficient			
		Model to data: Kirkwood–Riseman equation, HYDROPRO					
	J-couplings	Karplus equation	Backbone dihedral angles (ϕ); detects transient secondary structure.	Dihedral angles			
	Cross-correlated cross-relaxation	Data to model: correlation functions and Karplus-like equation	Dihedral angles based on correlated relaxation processes between two couplings.	Dihedral angles			
	RDCs	Modeling alignment and calculation of the coupling	Bond vector orientation; indicates transient structural elements and long-range order	Mutual orientation	External alignment (mechanically stressed gels, alignment media)		
SAXS	Scattering intensity as a function of the angle	CRYSOL/WAXSiS Pepsi-SAXS/FoXS	Provides global structural information	Global shapes and sizes, low-resolution structures	None required	In vitro	https://www.sasbdb.org/
SANS	Scattering intensity as a function of the angle	CRYSON/ pepsi-SANS	Complementary to SAXS	Global shapes and sizes, low-resolution structures	Deuteration	In vitro	https://www.sasbdb.org/
(sm)FRET	Transfer efficiency (fluorescence bursts or trajectories)	Förster equation + polymer models, molecular simulations>+ dye model (for example, FRET positioning and screening, Seidel), rotamer-library approaches (for example, FRETpredict)	Number of populations, FRET efficiencies, fluorescence lifetimes, fluorescence anisotropies	Intramolecular or intermolecular distance/distance distribution, conformational changes	Dye labeling	In vitro/in cell	Not applicable
	Fluorescence lifetime decay			Intramolecular or intermolecular distance distribution			
	Time correlation (nanosecond fluorescence correlation spectroscopy)			Distance relaxation time			

microscopy to observe immobilized molecules, or confocal spectroscopy to probe both freely diffusing and immobilized molecules. For IDPs, confocal-based smFRET avoids perturbations from immobilization and enables multiparameter detection (wavelength, lifetime, anisotropy, correlation)[54].

Proteins are subjected to site-specific labeling with donor–acceptor fluorophore pairs via cysteine residues or more advanced labeling strategies, such as nonnatural amino acids or intein-based ligation methods[55,56]. Heterogeneously labeled populations and different stoichiometries of intermolecular FRET can be resolved by alternating laser excitation or pulsed interleaved excitation[44,57]. The functional impact of labeling must be carefully assessed through control experiments, such as comparing the labeled and unlabeled IDP behavior in functional assays. Fluorophore mobility can be evaluated through time-resolved fluorescence anisotropy to ensure rotational freedom[43,44,54].

Quantitative analysis of smFRET data for IDPs. The FRET efficiency, E, for IDPs cannot be interpreted in terms of a fixed donor–acceptor distance. Instead, IDPs require analytical approaches that can account for the broad distributions, $P(r)$, of the inter-fluorophore distances r, and the dynamic timescales of protein and dye motions. Suitable models from polymer physics have commonly been used for describing global IDP features and to approximate $P(r)$[45]. Fluorescence lifetime measurements complement smFRET for accurate $P(r)$ determination. Two-dimensional plots of donor and acceptor fluorescence lifetime versus E can reveal whether a linear relationship exists (indicating fixed distances) or if deviations suggest broad and rapidly sampled distributions, offering a more stringent test of polymer models[43,44]. The integration with advanced computational approaches, including molecular simulations and Bayesian reweighting, can provide more detailed descriptions of $P(r)$ and deviations from simple polymer models, for instance in the presence of folded parts[46,58]. Nanosecond fluorescence correlation spectroscopy, combined with smFRET, enables the measurement of fast dynamics, including the reconfiguration times of disordered chains, which can be directly compared to simulations[45].

Important aspects for smFRET are to assess potential perturbations of the protein by fluorescent labeling, the analysis of complex distance distributions and the role of the relevant timescales of the measurement for signal averaging[45,59]. Advances in labeling technologies and integration with computational modeling, including an explicit representation of fluorophores, and complementary biophysical techniques make smFRET invaluable in integrative approaches of IDP ensemble determination[60,61].

SAS of X-rays and neutrons

Small-angle scattering (SAS) of X-rays (SAXS) and neutrons (SANS) have emerged as powerful techniques for the structural characterization of biomolecular systems in solution[62]. Despite being a low-resolution (1–2 nm) technique, SAS offers valuable structural information on the overall size and shape of biomolecules and biomolecular assemblies. In the context of IDPs, this information is key to constrain the ensemble description, and it is complementary to residue-level information derived from other techniques[63–65]. Major advances in beamline instrumentation, automatization, sample preparation and computational methods in the last decade have led to a tremendous increase in the application of SAS to structural biology[66]. The fast readout capabilities of current detectors enable kinetic monitoring of reactions across a broad timescale, from microseconds to hours, triggered by stopped-flow[67] or temperature jumps[68].

Although the conceptual framework of X-ray and neutron scattering as well as the strategies applied for their analysis are similar, these techniques differ in practical aspects, especially related to their sensitivity, which is much higher for SAXS[69,70]. The advantage of SANS arises from the different scattering power of nuclei, which is particularly large between the proton and the deuteron. Exploiting this isotope effect through contrast variation experiments of partially deuterated samples has been a key concept to enrich the structural content of SANS experiments[69,70].

Analysis of SAS data. The scattering profile of an IDP is the average of those arising from all coexisting conformations sampled in solution. As a consequence, SAS profiles measured for IDPs do not display features along the momentum transfer (q) range[63]. Traditionally, Kratky plots ($I(q) \times q^2$ as a function of q), especially in their dimensionless form[64], have been used to qualitatively identify (partly) disordered states and distinguish them from globular particles. The Kratky representation has the capacity to enhance particular features of scattering profiles, allowing an easier identification of different degrees of compactness[71].

The radius of gyration, R_g, which can be obtained from the smallest angles of a SAS curve using the Guinier approximation, is the most common descriptor to quantify the overall size of particles in solution. The experimental R_g is a single-value representation of the size of the molecule, which for disordered states represents an ensemble average over all accessible conformations of the IDP and its hydration layer. The most common quantitative interpretation of R_g for IDPs is based on Flory's equation, which relates it to the length of the protein chain through a power law ($R_g \propto N^{\upsilon}$), where N is the number of residues and υ is an exponential scaling factor. For chemically denatured proteins, a υ value of $\simeq$0.6 is expected[72]. However, according to theoretical models, IDPs are slightly more compact, with a υ value of 0.522 ± 0.01 (ref. 73). Recently, an approach has been developed to simultaneously derive the R_g and the υ value from a single SAXS profile[74], which has been used to connect the compactness of IDPs with their capacity for phase separation[36,75].

The pairwise distance distribution, $P(r)$, derived from the Fourier transformation of the SAS profile, provides a one-dimensional representation of the molecular structure, and it can also be used to qualitatively identify protein flexibility. The $P(r)$ also provides the maximum intramolecular distance, D_{max}, among all coexisting conformers. However, in the context of disordered proteins, D_{max} is not a robust parameter, and its quantitative interpretation is not recommended[76,77].

For IDPs, ensemble approaches are required, relying on two key ingredients: (i) accurate models of disordered states, and (ii) forward models with the capacity to robustly predict scattering properties including contributions from the solvent to the measured SAS data[78].

Other biophysical techniques

Other complementary experimental methods have also gained attention in the studying of IDP structural properties (Supplementary Table 1). Hydrogen deuterium exchange (HDX) relies on measuring the rate at which amide protons in the protein backbone exchange with deuterium in a heavy water solution, a process highly sensitive to structural fluctuations and hydrogen bonding. For IDPs, HDX by NMR spectroscopy or in particular by mass spectrometry (HDX-MS) provides valuable insights into disorder-to-order transitions, transient secondary-structure formation and conformational flexibility, making it a complementary technique to other structural methods such as NMR, smFRET or SAS. However, given the high exchange rates of IDPs, careful control of experimental conditions, such as pH, temperature and labeling times, becomes critical to ensure meaningful interpretation of the data[79]. Mass spectrometry-based techniques beyond HDX-MS, for example covalent labeling approaches such as hydroxyl radical footprinting or DEPC, and carboxyl or lysine-specific covalent modifications, provide complementary insights into IDP dynamics by irreversibly labeling solvent-exposed side chains on rapid timescales[80]. These methods capture transient and heterogeneous conformations that HDX may miss, offering residue-level resolution of side-chain exposure. Applications include detecting structural transitions during amyloid formation[81], mapping interaction interfaces[82] and identifying microenvironment-sensitive regions[83,84]. When combined

with modeling, these approaches enhance our ability to characterize the dynamic ensembles and functional states of IDPs.

Circular dichroism spectroscopy is a common technique for characterizing protein secondary structures by measuring the differential absorption of left- and right-circularly polarized light. Traditionally calibrated for globular proteins, circular dichroism spectroscopy has faced challenges in analyzing IDPs due to their weak and featureless spectra. Recent advancements have introduced new IDP reference datasets[85,86], enhancing the ability of this technique to detect conformational changes under various conditions. Despite these improvements, precise secondary-structure quantification of IDPs still remains a challenge.

Electron paramagnetic resonance spectroscopy, combined with site-directed spin labeling, is used to detect unpaired electrons and measure distance distributions between specific residues. It has emerged as a powerful technique for studying IDPs[87]. Electron paramagnetic resonance spectroscopy coupled with site-directed spin labeling is particularly useful for monitoring folding events and structural behavior, as it is not limited by protein size or system complexity[88]. The technique has been successfully applied to study disease-associated IDPs such as α-synuclein and tau, providing valuable insights into their conformational ensembles and interactions with the environment[87,89].

Integrative experimental modeling

Integrative experimental approaches rely on combining complementary experimental data to determine conformational ensembles. An analysis of the Protein Ensemble Database[90] shows that the most common hybrid approaches combine SAXS with NMR and/or smFRET. Notably, Gomes et al.[91] used experimental NMR and SAXS data to construct the conformational ensembles for Sic1 and phosphorylated Sic1, and subsequently used smFRET data as an independent validation criterion. In another recent study, Borthakur et al.[92] demonstrated that reweighted ensembles obtained from molecular dynamics simulations using different force fields converge to highly similar ensembles when incorporating extensive experimental data from NMR and SAXS. In addition, other combinations can be useful, such as SAXS, smFRET, fluorescence correlation spectroscopy and dynamic light scattering, as shown by Borgia et al.[93]. Such integrative studies illustrate how the information from different techniques is complementary.

Bridging experiments and theory: forward models

A critical element in translating experimental data into conformational ensembles is to define procedures, referred to as forward models, to calculate experimental observables from protein structures[94,95]. A major problem of forward models for IDPs is that most experimental methods provide data describing the average properties of proteins in solution, often over different timescales, rather than features of individual protein molecules, thus requiring a corresponding conformational averaging in the calculations[94,95]. Forward models estimating the experimental observables from generated models enable fitting experimental data obtained from various sources with a representative collection of conformations, as outlined in Table 1. Because the use of forward models influences the fitting procedure, selecting the appropriate model requires detailed understanding and considerations[96]. For instance, parameters of forward models need to be adjusted, ideally through self-consistent refinement against experimental datasets of both forward models and conformational ensembles[96–98]. Ultimately, experimental observations are influenced by both systematic and random errors, which must be accounted for to produce accurate and precise models[95].

To consider errors and the inherent variability of experimental observables, different Bayesian inference frameworks have been suggested[95,96]. Nonetheless, the development of more accurate and computationally efficient forward models and machine learning tools to account for different sources of error remains an active area of research.

Computational generation of conformational ensembles

Generating conformational ensembles through computational techniques is a critical step in integrative modeling of IDPs, providing atomic-level insight that complements experimental measurements. Recent progress has been driven by tighter integration between experimental and modeling efforts, where experimental data refine models and models aid in the interpretation of complex experiments[94]. Three main strategies are commonly used to generate conformational ensembles: knowledge-based methods, which draw on empirical patterns or structural fragments; physics-based simulations, which are based on biophysical principles to sample the conformational landscape; and machine learning-driven approaches, which infer structural features from data without explicit physical modeling. Each strategy offers distinct advantages, and their selection depends on the level of detail required, available data and modeling goals.

Knowledge-based methods

Knowledge-based methods (Table 2) generate conformational ensembles using heuristics or statistical patterns derived from known protein structures. These approaches often rely on fragment libraries, rotamer statistics or backbone angle distributions informed by structural databases. Examples of such methods include Flexible-Meccano[99], TraDES[100] and IDPConformerGenerator[101], which use fragments from nonredundant structural databases and statistical coil models to generate ensembles. Because they do not require energy calculations, they are computationally efficient and suitable for generating large conformational pools. These conformational collections can then be refined or reweighted based on experimental constraints to approximate statistical ensembles. Importantly, knowledge-based approaches are particularly useful when only limited experimental data are available, or when rapid conformational collection generation is needed for large-scale applications. A summary of representative methods and typical use cases is provided in Supplementary Table 2.

Physics-based methods

Physics-based approaches (Table 2) use molecular simulations to generate IDP ensembles. Since force fields originally developed for folded proteins often underestimate the flexibility and expanded conformations typical of disordered chains, IDP-specific force fields such as a99SB-disp[102] and Amber ff99SBws/ff03ws[103] have been developed to improve the balance between intramolecular and solvent interactions to better reflect IDP conformational preferences. Another challenge is sampling efficiency, as IDPs explore vast and shallow free-energy landscapes. Techniques like replica-exchange molecular dynamics[104], which run simulations in parallel at different temperatures to enhance conformational exploration, are commonly used to improve sampling. More recently, hybrid strategies that combine simulation with machine learning—for example, using machine learning-derived potentials to guide sampling—have emerged as promising tools[105,106]. Alternative frameworks such as hydrophobicity scale models[107] and CALVADOS[108,109], coarse-grained models parameterized against experimental data on IDPs and multidomain proteins, reduce computational cost while preserving some of the essential sequence-dependent behaviors. Beyond ensemble generation, physics-based methods increasingly contribute to design-oriented frameworks—from modeling the thermodynamic basis of multiphase condensates[110], to uncovering sequence–ensemble–function relationships in live cells[111], and enabling inverse design of IDRs with target ensemble properties[112–114]. Representative methods and applications are summarized in Supplementary Table 2.

https://doi.org/10.1038/s41592-026-03003-2

Table 2 | Comparison of computational strategies for the generation of conformational ensembles of IDPs

	Knowledge based	Physics based	Machine learning
Input	Protein sequence	Three-dimensional structural model	Protein sequence
	Structural fragments and SSPs (optional)	Force fields adapted for IDPs	
Core principle	Sampling backbone dihedrals using Protein Data Bank (PDB)-derived statistics or fragments	Simulates atomic motions over time using force fields	Learns statistical patterns from structural and/or experimental data to generate IDP ensembles from sequence
Resource/speed	Low; runs quickly on CPU with minimal setup	High; computationally intensive, often needs GPUs, HPC and force-field optimization	Moderate; fast inference after training, may require GPUs for large models
Output	Diverse ensembles reflecting backbone variability without including thermodynamic/kinetic information	Time-resolved or equilibrium ensembles with atomistic or coarse-grained resolution	Diverse coarse-grained/all-atom conformers sampled from a learned distribution
Typical use cases	Rapid conformer generation, SAXS ensemble preparation, fragment-based modeling	High-resolution structural refinement, validating experimental data (SAXS, NMR)	Sequence-to-ensemble modeling, large-scale IDP studies and synthetic ensemble generation

Machine learning methods

Machine learning approaches (Table 2) have recently emerged as an alternative strategy for generating conformational ensembles of IDPs. These methods aim to learn sequence–ensemble relationships directly from structural data, providing a way to overcome some of the limitations of traditional simulation-based techniques. For example, idpGAN[115] is a generative adversarial network trained on ensembles generated by coarse-grained molecular dynamics simulations, capable of producing novel ensembles with realistic $_{Rg}$. While still in early stages, machine learning-based models offer a promising route for efficient ensemble generation, especially when integrated with simulation-derived[116,117] and/or experimental data[118]. In addition to generating ensembles, machine learning and related statistical parameter-learning methods can be used to tune force-field parameters against experimental data[114,119], predicting IDP properties directly from sequence[4,6], designing novel IDP variants with desired properties[112,120] and predicting phase-separation propensities of IDPs[121]. Representative machine learning-based methods for computational ensemble generation are summarized in Supplementary Table 2.

Integration of computational models with experimental data

Experimental techniques such as NMR, SAXS and smFRET provide important insights into the behavior of IDPs, but these measurements typically report on averages over a wide range of rapidly fluctuating conformations. By contrast, computational methods—such as molecular simulations—can generate detailed conformational ensembles from a protein sequence. However, discrepancies often arise between simulations and experiments, reflecting inaccuracies in force fields, limited sampling or the nature of the experimental observable itself[122].

To address this aspect, an integrative modeling strategy is needed—one in which experimental data and computational ensembles inform and refine each other. The basic workflow (Fig. 2) involves generating an ensemble using a physics-based, knowledge-based or machine learning model, computing experimental observables from that ensemble using forward models, and comparing them with actual experimental measurements. When agreement is poor, the ensemble can be refined or reweighted so that its average properties better match the data.

Two main classes of approaches are available for this purpose. The first is based on maximum entropy[123], a foundational concept in statistical mechanics for generating the most unbiased ensemble consistent with known constraints. In its simplest form, and in the absence of experimental data, structural ensembles follow the Boltzmann distribution: $P_i = \frac{1}{Z}e^{-\beta E_i}$ where E_i is the energy of conformation i, β is the inverse thermal energy, and Z is the partition function. However, when experimental observables are introduced, such as NMR chemical shifts or SAXS profiles, this framework is generalized to a Gibbs distribution: $P_i = \frac{1}{Z}e^{-\Sigma_k \beta_k E_{ik}}$. Here, E_{ik} represents an effective energy term for the deviation of conformation i from experimental observable k, and β_k (a Lagrange multiplier) adjusts the weight of that constraint. This formulation ensures the structural ensemble remains as close as possible to the original distribution while still fulfilling the experimental data. In practice, this statistical foundation, together with the principles from Bayesian statistics, underlies a number of maximum-entropy-based methods such as Bayesian/maximum entropy (BME)[124], BioEn[125] and metainference[95]. These approaches implement the principle either by reweighting existing conformers post hoc, or by applying biasing forces during simulations to guide sampling. Such techniques are especially effective for IDPs, whose native states are characterized by extensive structural heterogeneity that must be preserved during model refinement.

The second category, known as maximum parsimony methods, seeks to identify the smallest subset of conformers from a large pool that can adequately explain the experimental data, minimizing structural complexity. In contrast to maximum entropy, maximum parsimony methods aim to simplify the conformational collection by selecting or reweighting structures to maximize agreement with experimental observations while minimizing the size of the conformational collection. These approaches, such as EOM[126] and ASTEROIDS[127], are particularly useful when only a few conformational states are dominant and are thus most suitable for low-entropy systems with limited conformational heterogeneity, where a description in terms of statistical ensemble is not required.

These integrative strategies yield experimentally validated, physically realistic ensembles. Representative techniques for integration of experimental data are provided in Supplementary Table 3.

Hybrid computational techniques

Some computational methods for modeling IDPs leverage complementary modeling strategies. These hybrid approaches (Supplementary Table 2) integrate complementary ensemble generation techniques, or couple ensemble generation directly with experimental data integration strategies. One strategy involves combining physics-based and knowledge-based approaches to enhance sampling efficiency and structural diversity. For example, FastFloppyTail[128] uses fragment-based backbone sampling alongside energy-based refinement. Other techniques couple machine learning with physics-based modeling, such as AlphaFold–Metainference[106] and bAIes[105], which refines deep learning predictions from AlphaFold via Bayesian ensemble inference and molecular simulation. A different class of hybrid

https://doi.org/10.1038/s41592-026-03003-2

methods links ensemble generation with experimentally data-driven refinement. For instance, DynamICE[118] integrates machine learning with maximum-entropy principles to iteratively optimize ensemble structures based on NMR data. These flexible and composable pipelines offer practical advantages when addressing the complexity of IDP ensembles, particularly in cases where no single modeling paradigm is sufficient.

Open challenges in conformational ensemble generation

Despite recent advances, several challenges remain in generating conformational ensembles[122]. First, force-field accuracy continues to be a critical limitation. While parametrizations using experimental data and quantum chemistry calculations are continuously improving their accuracy, current force fields still rely on rather simple functional forms established decades ago, and fail to describe subtle interactions, such as those arising from polarization effects, especially in complex or highly flexible biomolecules. Progress in developing more accurate force fields may require closer collaboration between experimental and computational researchers and the development of top-down approaches, including the adoption of machine learning methods[108,119,129].

Second, the optimal integration of experimental data into simulations is still an open problem[95,122]. Many forward models used to translate experimental data into simulation restraints are limited by their assumptions and approximations. Accounting for the ensemble-averaged nature of most experimental observables on IDPs, such as those derived from NMR or smFRET, or the effect of the hydration for SAS, is critical for accurate modeling. Robust frameworks that address uncertainties in both experimental data and forward models are essential to bridge this gap[95,122]. In the absence of ground-truth conformational ensembles, such frameworks require experimental data from orthogonal techniques and for different proteins to self-consistently select, refine and validate forward models[96,98,130]. These experimental data are typically insufficient to describe a unique conformational ensemble, with the final result dependent on the computational model used to generate the ensemble.

Third, the efficient sampling of conformational space also remains a critical bottleneck. Insufficient sampling can lead to incomplete or biased conclusions, making it crucial to assess convergence rigorously. Advancements in some techniques, such as accelerated molecular dynamics and Markov state models[131,132], offer potential solutions but require widespread adoption and careful validation.

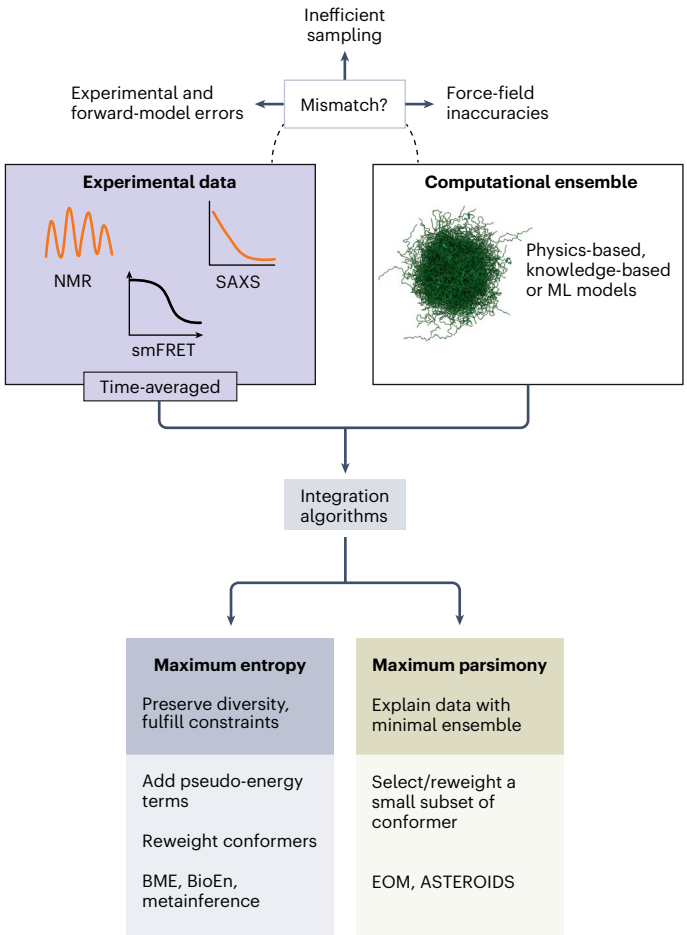

Fig. 2 | Overview of integrative modeling strategies for IDPs. Experimental methods such as NMR, SAXS and smFRET provide averaged data across many conformations, while computational models generate detailed structural ensembles. When the two disagree, for example due to limited sampling, force-field inaccuracies or experimental noise, different strategies can be used to improve agreement. These include maximum-entropy methods that adjust structural ensemble weights and maximum parsimony methods that generate conformational collections by selecting a minimal subset of structures. These strategies help align computational models with experimental data. Figure created in BioRender; Ghafouri, H. https://biorender.com/194xtx1 (2025).

Conformational ensemble validation and comparison

Comparison of conformational ensembles

The determination of an IDP ensemble from sparse experimental data is a mathematically underdetermined problem, leading to multiple solutions. Hence, the comparison of these ensembles may be critical for validating them (see next section), and/or for deriving mechanistic insights by identifying functional correlates (for example, binding regions, dynamic linkers), comparing homologous IDPs and assessing the influence of solution conditions. As conformational ensemble comparison methods for folded proteins[133] are difficult to generalize to IDPs, various approaches have been developed in recent years. One common strategy is to represent a conformational ensemble by a single scalar that quantifies its conformational heterogeneity[134], and differences in this value can be used to compare two conformational ensembles. While this metric is easy to interpret, it offers only a limited view of the differences between conformational ensembles and lacks the resolution to capture more local structural or dynamical variations. A more sophisticated approach involves analyzing the differences in distance distributions of individual residue pairs and assessing their statistical significance between two conformational ensembles[135]. However, given the vast conformational variability of IDPs, it is essential to consider both average properties and their distributions. Indeed, reducing IDP conformational descriptors to their mean can lead to major information loss. Therefore, several methods have been proposed for extending comparative structural analyses to a distributional framework, using various similarity measures to compare probability distribution functions, such as the Kullback–Leibler and the Jensen–Shannon divergence[133,135,136], Hellinger distance[137] or the Wasserstein distance[138]. Among these, the Wasserstein distance is particularly appealing for its incorporation of the geometry of the underlying space, although it is more computationally demanding than the others. In this framework, different descriptors can be used to characterize conformations inside each ensemble and to compute pairwise distances. The most natural one is to use atomic coordinates and RMSD[133]; however, the required structural superposition hinders its application to IDPs. To circumvent this problem, other descriptors such as torsion angles[139] or other local structural properties[136] can be considered. For a more comprehensive comparison, local and global structural descriptors can be taken into account in a unified way[138]. Other approaches for the comparative analysis of conformational ensembles, such as methods incorporating topology concepts[140] or the identification of local energy traps at the residue level[141], have been explored. Supplementary Table 4 summarizes conformational ensemble comparison methods.

Validation of conformational ensembles

Validating conformational ensembles of IDPs is challenging, as their accuracy and precision are difficult to establish. Nonetheless, objective criteria can be applied, generally relying on orthogonal experimental data and emphasizing the importance of integrative approaches.

Validation typically begins with basic stereochemical checks to ensure that each conformation follows physicochemical rules. These include proper bond lengths, torsion angles, Ramachandran distributions and the absence of atomic clashes. Such conditions are not always satisfied in Protein Ensemble Database ensembles[90]. The next step is to verify that ensembles reproduce global structural parameters derived from experiments like SAS and smFRET, or estimated from sequence using polymer-physical principles[4,45,142]. These include R_g, end-to-end distance, asphericity and scaling exponents (υ)[143,144]. Because global parameters can be affected by secondary structure and long-range contacts, validation should proceed to more local descriptors, including smFRET-derived and PRE-derived distances, inter-residue contact probabilities[145,146], secondary-structure content from circular dichroism or NMR and residue-specific conformational preferences obtained from NMR observables such as chemical shifts, RDCs and nuclear Overhauser effects.

Robustness is another essential criterion. Ensembles that change substantially when subsets of input data are removed indicate limited accuracy[122,147]. By contrast, predictive power, that is, the ability to anticipate independent experimental observables, provides strong validation[148].

Functional relevance is equally important. Ensembles should capture biologically meaningful features such as disorder-to-order transitions and the presence of bound-like states in the unbound ensemble[149]. They may also reflect evolutionary conservation of global dimensions or correlations between compaction and Gene Ontology functional descriptors[4,5]. In disease contexts, ensembles can help explain mechanisms or guide therapeutic design, for example by predicting small-molecule binding and supporting structure–activity relationship studies[150–152].

Finally, most ensembles are generated under in vitro conditions, which may not fully represent in-cell conformations. The ultimate benchmark for validation will, therefore, come from cellular structural data, such as in-cell NMR or smFRET[50,153], which remain in early stages of development[40,154].

Roadmap for conformational ensemble determination

The determination of conformational ensembles of IDPs is at a critical moment: methodologies are expanding rapidly, but standardized practices for validation, comparison and application remain elusive. To address these challenges, we propose a four-pronged roadmap: establishing a benchmarking infrastructure, developing robust approaches for uncertainty quantification, incorporating nonequilibrium and kinetic aspects, and offering practical guidelines for method selection.

IDP Ensemble Benchmarking Challenge

A major step toward advancing ensemble modeling is the creation of a transparent and standardized benchmarking initiative. Inspired by the success of CASP in protein structure prediction[155] and CAID in disorder prediction[156], we propose the IDP Ensemble Benchmarking Challenge (IDP-Bench), a recurring, community-driven assessment platform (Supplementary Fig. 1). Its biennial cycle will include selection of diverse experimental datasets by an independent committee, submission of ensemble predictions by participating groups, automated scoring against withheld validation data and continuous dissemination of results through a dedicated website.

The first edition will focus on well-characterized IDPs such as α-synuclein, Sic1, the K18 repeat and full-length tau, p27Kip1 and the measles-virus NTAIL domain, which together cover diverse sequence features, biological functions and experimental accessibility. These proteins have extensive datasets, including SAXS, PRE, RDC, smFRET and HDX-MS. Scoring will combine global metrics such as χ^2 for SAXS profiles and Kullback–Leibler divergence for distance distributions with local measures such as PRE RMSE, RDC Q-factors and Wasserstein distances for smFRET (Supplementary Table 5). These will be combined into a weighted composite score, with scripts and error models released as open-source tools. To test predictive capability more rigorously, blind datasets such as SAXS or NMR under defined conditions will be introduced in a second phase. IDP-Bench will provide a sustainable benchmarking ecosystem that promotes transparency, drives innovation and enables long-term progress tracking.

Uncertainty in conformational ensemble determination

Benchmarking requires not only standardized data and metrics but also systematic treatment of uncertainty. We propose that uncertainty quantification be integrated directly into the IDP-Bench framework. Supplementary Fig. 2 summarizes the main error sources across experimental observables and serves as a guide for reproducibility and model fitting. Forward-model errors must also be included. For example, SPARTA+ predictions of backbone Cα chemical shifts have a standard deviation of about 1 ppm on its training dataset[157], and SAXS predictions with CRYSOL can deviate systematically due to hydration shell modeling and background corrections[158,159]. Where empirical error estimates are lacking, bootstrapping over modeling parameters such as fluorophore grids or rotamer libraries can provide confidence intervals.

The scoring pipeline will report both standard metrics and statistical descriptors such as reduced χ^2, residual distributions and Bayes factors, allowing discrimination between genuine fits and overfitting. Transparency will be enforced by requiring participants to submit a checklist detailing experimental uncertainties, sources of forward-model error, bootstrap or posterior distributions of fitted parameters, and treatment of outliers. By embedding uncertainty quantification at every stage, ensemble quality can be judged not only in absolute terms but also relative to experimental noise and modeling limitations.

Dynamic properties and nonequilibrium behavior of IDPs

Many IDPs act through transient interactions and conformational switching that are not captured by equilibrium models. Progress in time-resolved techniques, including X-ray crystallography with free-electron lasers[160], real-time NMR[161], time-resolved and single-molecule FRET[162], time-resolved HDX-MS[163] and SAXS[164] and liquid-state electron microscopy[165] now enables access to kinetic processes. These measurements can be used as restraints for simulations that reconstruct the time evolution of ensembles.

Theoretical frameworks such as maximum entropy and its dynamical extension, maximum caliber, allow the inference of dynamic behavior consistent with experimental observations[166,167]. These approaches are still in their early stages but provide a path toward dynamic ensemble models that more realistically capture time-dependent IDP function.

Guidelines for method selection

To support practitioners, we propose a decision framework for method selection, summarized in Supplementary Fig. 3 and Supplementary Tables 2 and 3. The process begins with evaluation of available experimental data. When no structural information exists, molecular dynamics simulations can provide baseline hypotheses. For systems constrained only by local data, knowledge-based or machine learning generators coupled with reweighting are recommended. When both local and global data such as smFRET and SAXS are available, hybrid restrained simulations or Bayesian and maximum-entropy approaches offer the best balance between fidelity and generalizability.

Biological objectives should also guide model resolution. All-atom ensembles are preferred for site-specific predictions such as binding

interfaces and mutational effects, while coarse-grained models are more suitable for large-scale processes such as phase behavior or scaling laws, where computational efficiency and statistical representativeness are critical. Resource availability further shapes method choice. On a desktop workstation, knowledge-based sampling or accelerated Monte Carlo approaches are most practical. Access to modest GPU clusters allows replica-exchange simulations or hybrid reweighting, whereas high-performance computing facilities make possible extensive all-atom replica simulations and advanced machine learning refinement strategies.

Conclusion

In the face of growing interest in disordered proteins and the understating of their structural properties, this Perspective establishes a comprehensive and practical framework to guide IDP ensemble determination, benchmarking and interpretation. By integrating community expertise across experimental and computational domains, we chart a roadmap for IDP ensemble determination, emphasize the need for uncertainty quantification and propose actionable benchmarking strategies. To implement this roadmap, we established the IDP Ensemble Benchmarking Challenge, following the examples of CASP and CAID, which greatly contributed to major advances in computational structural biology. This collaborative effort not only provides clarity on the current landscape of conformational ensemble modeling but also defines a shared vision for its future. As the field moves toward consensus and interoperability, we hope this work will serve as both a reference and a call to action, catalyzing rigorous, reproducible and biologically relevant studies of disordered protein conformational space.

References

1. Piovesan, D. et al. MOBIDB in 2025: integrating ensemble properties and function annotations for intrinsically disordered proteins. *Nucleic Acids Res.* **53**, D495–D503 (2025).
2. Holehouse, A. S. & Kragelund, B. B. The molecular basis for cellular function of intrinsically disordered protein regions. *Nat. Rev. Mol. Cell Biol.* **25**, 187–211 (2024).
3. Waterbury, A. L. et al. An autoinhibitory switch of the LSD1 disordered region controls enhancer silencing. *Mol. Cell* **84**, 2238–2254 (2024).
4. Tesei, G. et al. Conformational ensembles of the human intrinsically disordered proteome. *Nature* **626**, 897–904 (2024).
5. González-Foutel, N. S. et al. Conformational buffering underlies functional selection in intrinsically disordered protein regions. *Nat. Struct. Mol. Biol.* **29**, 781–790 (2022).
6. Lotthammer, J. M., Ginell, G. M., Griffith, D., Emenecker, R. J. & Holehouse, A. S. Direct prediction of intrinsically disordered protein conformational properties from sequences. *Nat. Methods* https://doi.org/10.1038/s41592-023-02159-5 (2024).
7. Abragam, A. & Hebel, L. C. The principles of nuclear magnetism. *Am. J. Phys.* **29**, 860–861 (1961).
8. Alderson, T. R., Lee, J. H., Charlier, C., Ying, J. & Bax, A. Propensity for *cis*-proline formation in unfolded proteins. *Chembiochem* **19**, 37–42 (2018).
9. Murrali, M. G., Piai, A., Bermel, W., Felli, I. C. & Pierattelli, R. Proline fingerprint in intrinsically disordered proteins. *Chembiochem* **19**, 1625–1629 (2018).
10. Mateos, B. et al. The ambivalent role of proline residues in an intrinsically disordered protein: from disorder promoters to compaction facilitators. *J. Mol. Biol.* **432**, 3093–3111 (2020).
11. Redfield, C. Using nuclear magnetic resonance spectroscopy to study molten globule states of proteins. *Methods* **34**, 121–132 (2004).
12. Alderson, T. R. & Kay, L. E. Unveiling invisible protein states with NMR spectroscopy. *Curr. Opin. Struct. Biol.* **60**, 39–49 (2020).
13. Marsh, J. A., Singh, V. K., Jia, Z. & Forman-Kay, J. D. Sensitivity of secondary structure propensities to sequence differences between alpha- and gamma-synuclein: implications for fibrillation. *Protein Sci.* **15**, 2795–2804 (2006).
14. Camilloni, C., De Simone, A., Vranken, W. F. & Vendruscolo, M. Determination of secondary structure populations in disordered states of proteins using nuclear magnetic resonance chemical shifts. *Biochemistry* **51**, 2224–2231 (2012).
15. Nielsen, J. T. & Mulder, F. A. A. POTENCI: prediction of temperature, neighbor and pH-corrected chemical shifts for intrinsically disordered proteins. *J. Biomol. NMR* **70**, 141–165 (2018).
16. Neal, S., Nip, A. M., Zhang, H. & Wishart, D. S. Rapid and accurate calculation of protein ^{1}H, ^{13}C and ^{15}N chemical shifts. *J. Biomol. NMR* **26**, 215–240 (2003).
17. Shen, Y. & Bax, A. SPARTA+: a modest improvement in empirical NMR chemical shift prediction by means of an artificial neural network. *J. Biomol. NMR* **48**, 13–22 (2010).
18. Li, D. -W. & Brüschweiler, R. PPM: a side-chain and backbone chemical shift predictor for the assessment of protein conformational ensembles. *J. Biomol. NMR* **54**, 257–265 (2012).
19. Kohlhoff, K. J., Robustelli, P., Cavalli, A., Salvatella, X. & Vendruscolo, M. Fast and accurate predictions of protein NMR chemical shifts from interatomic distances. *J. Am. Chem. Soc.* **131**, 13894–13895 (2009).
20. Karplus, M. Contact electron-spin coupling of nuclear magnetic moments. *J. Chem. Phys.* **30**, 11–15 (1959).
21. Salvador, P. Dependencies of *J*-couplings upon dihedral angles on proteins. *Annu. Rep. NMR Spectrosc.* 81, 185–227 (2014).
22. Reif, B., Hennig, M. & Griesinger, C. Direct measurement of angles between bond vectors in high-resolution NMR. *Science* **276**, 1230–1233 (1997).
23. Braun, D. et al. Local structure propensities in disordered proteins from cross-correlated NMR spin relaxation. *J. Biomol. NMR* **79**, 115–127 (2025).
24. Marsh, J. A., Baker, J. M. R., Tollinger, M. & Forman-Kay, J. D. Calculation of residual dipolar couplings from disordered state ensembles using local alignment. *J. Am. Chem. Soc.* **130**, 7804–7805 (2008).
25. Delaforge, E., Cordeiro, T. N., Bernadó, P. & Sibille, N. Conformational characterization of intrinsically disordered proteins and its biological significance. in *Modern Magnetic Resonance* (ed. Webb, G. A.) 381–399 (Springer International Publishing, 2018). https://doi.org/10.1007/978-3-319-28388-3_52
26. Camilloni, C. & Vendruscolo, M. A tensor-free method for the structural and dynamical refinement of proteins using residual dipolar couplings. *J. Phys. Chem. B* **119**, 653–661 (2015).
27. Bernadó, P. et al. A structural model for unfolded proteins from residual dipolar couplings and small-angle X-ray scattering. *Proc. Natl. Acad. Sci. USA* **102**, 17002–17007 (2005).
28. Abyzov, A. et al. Identification of dynamic modes in an intrinsically disordered protein using temperature-dependent NMR relaxation. *J. Am. Chem. Soc.* **138**, 6240–6251 (2016).
29. Adamski, W. et al. A unified description of intrinsically disordered protein dynamics under physiological conditions using NMR spectroscopy. *J. Am. Chem. Soc.* **141**, 17817–1782 9 (2019).
30. Salvi, N., Abyzov, A. & Blackledge, M. Multi-timescale dynamics in intrinsically disordered proteins from NMR relaxation and molecular simulation. *J. Phys. Chem. Lett.* **7**, 2483–2489 (2016).
31. Bertoncini, C. W. et al. Release of long-range tertiary interactions potentiates aggregation of natively unstructured alpha-synuclein. *Proc. Natl. Acad. Sci. USA* **102**, 1430–1435 (2005).

32. Mateos, B., Konrat, R., Pierattelli, R. & Felli, I. C. NMR characterization of long-range contacts in intrinsically disordered proteins from paramagnetic relaxation enhancement in ^{13}C direct-detection experiments. *Chembiochem* **20**, 335–339 (2019).
33. Kawasaki, R. & Tate, S. -I. Impact of the hereditary P301L mutation on the correlated conformational dynamics of human tau protein revealed by the paramagnetic relaxation enhancement NMR experiments. *Int. J. Mol. Sci.* **21**, 3920 (2020).
34. Salmon, L. et al. NMR characterization of long-range order in intrinsically disordered proteins. *J. Am. Chem. Soc.* **132**, 8407–8418 (2010).
35. Cordeiro, T. N. et al. Interplay of protein disorder in retinoic acid receptor heterodimer and its corepressor regulates gene expression. *Structure* **27**, 1270–1285 (2019).
36. Du, Z. et al. The sequence-structure-function relationship of intrinsic ERα disorder. *Nature* **638**, 1130–1138 (2025).
37. Kurzbach, D. et al. NMR probing and visualization of correlated structural fluctuations in intrinsically disordered proteins. *Phys. Chem. Chem. Phys.* **19**, 10651–10656 (2017).
38. Serber, Z., Ledwidge, R., Miller, S. M. & Dötsch, V. Evaluation of parameters critical to observing proteins inside living *Escherichia coli* by in-cell NMR spectroscopy. *J. Am. Chem. Soc.* **123**, 8895–8901 (2001).
39. Serber, Z. et al. High-resolution macromolecular NMR spectroscopy inside living cells. *J. Am. Chem. Soc.* **123**, 2446–2447 (2001).
40. Theillet, F. -X. et al. Structural disorder of monomeric α-synuclein persists in mammalian cells. *Nature* **530**, 45–50 (2016).
41. Felli, I. C., Gonnelli, L. & Pierattelli, R. In-cell ^{13}C NMR spectroscopy for the study of intrinsically disordered proteins. *Nat. Protoc.* **9**, 2005–2016 (2014).
42. Lerner, E. et al. FRET-based dynamic structural biology: challenges, perspectives and an appeal for open-science practices. *eLife* **10**, e60416 (2021).
43. Metskas, L. A. & Rhoades, E. Single-molecule FRET of intrinsically disordered proteins. *Annu. Rev. Phys. Chem.* **71**, 391–414 (2020).
44. Chowdhury, A., Nettels, D. & Schuler, B. Interaction dynamics of intrinsically disordered proteins from single-molecule spectroscopy. *Annu. Rev. Biophys.* **52**, 433–462 (2023).
45. Schuler, B., Soranno, A., Hofmann, H. & Nettels, D. Single-molecule FRET spectroscopy and the polymer physics of unfolded and intrinsically disordered proteins. *Annu. Rev. Biophys.* **45**, 207–231 (2016).
46. Holmstrom, E. D. et al. Accurate transfer efficiencies, distance distributions, and ensembles of unfolded and intrinsically disordered proteins from single-molecule FRET. *Methods Enzymol.* **611**, 287–325 (2018).
47. Zosel, F., Soranno, A., Buholzer, K. J., Nettels, D. & Schuler, B. Depletion interactions modulate the binding between disordered proteins in crowded environments. *Proc. Natl. Acad. Sci. USA* **117**, 13480–13489 (2020).
48. Galvanetto, N. et al. Extreme dynamics in a biomolecular condensate. *Nature* **619**, 876–883 (2023).
49. Nasir, I., Onuchic, P. L., Labra, S. R. & Deniz, A. A. Single-molecule fluorescence studies of intrinsically disordered proteins and liquid phase separation. *Biochim. Biophys. Acta Proteins Proteom.* **1867**, 980–987 (2019).
50. Sustarsic, M. & Kapanidis, A. N. Taking the ruler to the jungle: single-molecule FRET for understanding biomolecular structure and dynamics in live cells. *Curr. Opin. Struct. Biol.* **34**, 52–59 (2015).
51. Ferreon, A. C. M., Gambin, Y., Lemke, E. A. & Deniz, A. A. Interplay of alpha-synuclein binding and conformational switching probed by single-molecule fluorescence. *Proc. Natl. Acad. Sci. USA* **106**, 5645–5650 (2009).
52. Melo, A. M. et al. A functional role for intrinsic disorder in the tau-tubulin complex. *Proc. Natl. Acad. Sci. USA* **113**, 14336–14341 (2016).
53. Elbaum-Garfinkle, S. & Rhoades, E. Identification of an aggregation-prone structure of tau. *J. Am. Chem. Soc.* **134**, 16607–16613 (2012).
54. Sisamakis, E., Valeri, A., Kalinin, S., Rothwell, P. J. & Seidel, C. A. M. Accurate single-molecule FRET studies using multiparameter fluorescence detection. *Methods Enzymol.* **475**, 455–514 (2010).
55. Nikić, I. & Lemke, E. A. Genetic code expansion enabled site-specific dual-color protein labeling: superresolution microscopy and beyond. *Curr. Opin. Chem. Biol.* **28**, 164–173 (2015).
56. Zosel, F., Holla, A. & Schuler, B. Labeling of proteins for single-molecule fluorescence spectroscopy. *Methods Mol. Biol.* **2376**, 207–233 (2022).
57. Hohlbein, J., Craggs, T. D. & Cordes, T. Alternating-laser excitation: single-molecule FRET and beyond. *Chem. Soc. Rev.* **43**, 1156–1171 (2014).
58. Hofmann, H. Understanding disordered and unfolded proteins using single-molecule FRET and polymer theory. *Methods. Appl. Fluoresc.* **4**, 042003 (2016).
59. Miller, J. J. et al. Accounting for fast vs slow exchange in single molecule FRET experiments reveals hidden conformational states. *J. Chem. Theory Comput.* **20**, 10339–10349 (2024).
60. Naudi-Fabra, S., Tengo, M., Jensen, M. R., Blackledge, M. & Milles, S. Quantitative description of intrinsically disordered proteins using single-molecule FRET, NMR, and SAXS. *J. Am. Chem. Soc.* **143**, 20109–20121 (2021).
61. Nettels, D. et al. Single-molecule FRET for probing nanoscale biomolecular dynamics. *Nat. Rev. Phys.* **6**, 587–605 (2024).
62. Koch, M. H., Vachette, P. & Svergun, D. I. Small-angle scattering: a view on the properties, structures and structural changes of biological macromolecules in solution. *Q. Rev. Biophys.* **36**, 147–227 (2003).
63. Bernadó, P. & Svergun, D. I. Structural analysis of intrinsically disordered proteins by small-angle X-ray scattering. *Mol. Biosyst.* **8**, 151–167 (2012).
64. Receveur-Brechot, V. & Durand, D. How random are intrinsically disordered proteins? A small angle scattering perspective. *Curr. Protein Pept. Sci.* **13**, 55–75 (2012).
65. Kikhney, A. G. & Svergun, D. I. A practical guide to small angle X-ray scattering (SAXS) of flexible and intrinsically disordered proteins. *FEBS Lett.* **589**, 2570–2577 (2015).
66. Trewhella, J. Recent advances in small-angle scattering and its expanding impact in structural biology. *Structure* **30**, 15–23 (2022).
67. Konuma, T. et al. Highly collapsed conformation of the initial folding intermediates of β-lactoglobulin with non-native α-helix. *J. Mol. Biol.* **427**, 3158–3165 (2015).
68. Shkumatov, A. V., Chinnathambi, S., Mandelkow, E. & Svergun, D. I. Structural memory of natively unfolded tau protein detected by small-angle X-ray scattering. *Proteins* **79**, 2122–2131 (2011).
69. Mahieu, E. & Gabel, F. Biological small-angle neutron scattering: recent results and development. *Acta Crystallogr. D Struct. Biol.* **74**, 715–726 (2018).
70. Krueger, S. Small-angle neutron scattering contrast variation studies of biological complexes: challenges and triumphs. *Curr. Opin. Struct. Biol.* **74**, 102375 (2022).
71. Doniach, S. Changes in biomolecular conformation seen by small angle X-ray scattering. *Chem. Rev.* **101**, 1763–1778 (2001).
72. Flory, P. J. *Principles of Polymer Chemistry* (Cornell University Press, 1953).
73. Bernadó, P. & Blackledge, M. A self-consistent description of the conformational behavior of chemically denatured proteins from NMR and small angle scattering. *Biophys. J.* **97**, 2839–2845 (2009).

74. Riback, J. A. et al. Innovative scattering analysis shows that hydrophobic disordered proteins are expanded in water. *Science* **358**, 238–241 (2017).
75. Bremer, A. et al. Deciphering how naturally occurring sequence features impact the phase behaviours of disordered prion-like domains. *Nat. Chem.* **14**, 196–207 (2022).
76. Heller, W. T. Influence of multiple well defined conformations on small-angle scattering of proteins in solution. *Acta Crystallogr. D Biol. Crystallogr.* **61**, 33–44 (2005).
77. Bernadó, P. Effect of interdomain dynamics on the structure determination of modular proteins by small-angle scattering. *Eur. Biophys. J.* **39**, 769–780 (2010).
78. Cordeiro, T. N. et al. Small-angle scattering studies of intrinsically disordered proteins and their complexes. *Curr. Opin. Struct. Biol.* **42**, 15–23 (2017).
79. Masson, G. R. et al. Recommendations for performing, interpreting and reporting hydrogen deuterium exchange mass spectrometry (HDX-MS) experiments. *Nat. Methods* **16**, 595–602 (2019).
80. Mitra, G. Emerging role of mass spectrometry-based structural proteomics in elucidating intrinsic disorder in proteins. *Proteomics* **21**, e2000011 (2021).
81. Beveridge, R. & Calabrese, A. N. Structural proteomics methods to interrogate the conformations and dynamics of intrinsically disordered proteins. *Front. Chem.* **9**, 603639 (2021).
82. Pan, X., Tran, T., Kirsch, Z. J., Thompson, L. K. & Vachet, R. W. Diethylpyrocarbonate-based covalent labeling mass spectrometry of protein interactions in a membrane complex system. *J. Am. Soc. Mass. Spectrom.* **34**, 82–91 (2023).
83. Biehn, S. E., Limpikirati, P., Vachet, R. W. & Lindert, S. Utilization of hydrophobic microenvironment sensitivity in diethylpyrocarbonate labeling for protein structure prediction. *Anal. Chem.* **93**, 8188–8195 (2021).
84. Barth, M., Bender, J., Kundlacz, T. & Schmidt, C. Evaluation of NHS-acetate and DEPC labelling for determination of solvent accessible amino acid residues in protein complexes. *J. Proteomics* **222**, 103793 (2020).
85. Miles, A. J., Drew, E. D. & Wallace, B. A. DichroIDP: a method for analyses of intrinsically disordered proteins using circular dichroism spectroscopy. *Commun. Biol.* **6**, 823 (2023).
86. Nagy, G., Hoffmann, S. V., Jones, N. C. & Grubmüller, H. Reference data set for circular dichroism spectroscopy comprised of validated intrinsically disordered protein models. *Appl. Spectrosc.* **78**, 897–911 (2024).
87. Drescher, M. EPR in protein science: intrinsically disordered proteins. *Top. Curr. Chem.* **321**, 91–119 (2012).
88. Le Breton, N. et al. Exploring intrinsically disordered proteins using site-directed spin labeling electron paramagnetic resonance spectroscopy. *Front. Mol. Biosci.* **2**, 21 (2015).
89. Weickert, S., Cattani, J., & Drescher, M. Intrinsically disordered proteins (IDPs) studied by EPR and in-cell EPR. In *Electron Paramagnetic Resonance* Vol. 26 (eds Chechik, V. & Murphy, D. M.) 1–37 (2018); https://doi.org/10.1039/9781788013888-00001
90. Ghafouri, H. et al. PED in 2024: improving the community deposition of structural ensembles for intrinsically disordered proteins. *Nucleic Acids Res.* **52**, D536–D544 (2024).
91. Gomes, G. -N. W. et al. Conformational ensembles of an intrinsically disordered protein consistent with NMR, SAXS, and single-molecule FRET. *J. Am. Chem. Soc.* **142**, 15697–15710 (2020).
92. Borthakur, K. et al. Determining accurate conformational ensembles of intrinsically disordered proteins at atomic resolution. *Nat. Commun.* **16**, 9036 (2025).
93. Borgia, A. et al. Consistent view of polypeptide chain expansion in chemical denaturants from multiple experimental methods. *J. Am. Chem. Soc.* **138**, 11714–11726 (2016).
94. Bottaro, S. & Lindorff-Larsen, K. Biophysical experiments and biomolecular simulations: a perfect match?. *Science* **361**, 355–360 (2018).
95. Bonomi, M., Camilloni, C., Cavalli, A. & Vendruscolo, M. Metainference: a Bayesian inference method for heterogeneous systems. *Sci. Adv.* **2**, e1501177 (2016).
96. Pesce, F. & Lindorff-Larsen, K. Refining conformational ensembles of flexible proteins against small-angle X-ray scattering data. *Biophys. J.* **121**, 1576–1579 (2022).
97. Lindorff-Larsen, K., Best, R. B. & Vendruscolo, M. Interpreting dynamically-averaged scalar couplings in proteins. *J. Biomol. NMR* **32**, 273–280 (2005).
98. Lindorff-Larsen, K. & Kragelund, B. B. On the potential of machine learning to examine the relationship between sequence, structure, dynamics and function of intrinsically disordered proteins. *J. Mol. Biol.* **433**, 167196 (2021).
99. Ozenne, V. et al. Flexible-meccano: a tool for the generation of explicit ensemble descriptions of intrinsically disordered proteins and their associated experimental observables. *Bioinformatics* **28**, 1463–1470 (2012).
100. Feldman, H. J. & Hogue, C. W. V. Probabilistic sampling of protein conformations: new hope for brute force?. *Proteins* **46**, 8–23 (2002).
101. Teixeira, J. M. C. et al. IDPConformerGenerator: a flexible software suite for sampling the conformational space of disordered protein states. *J. Phys. Chem. A* **126**, 5985–6003 (2022).
102. Robustelli, P., Piana, S. & Shaw, D. E. Developing a molecular dynamics force field for both folded and disordered protein states. *Proc. Natl. Acad. Sci. USA* **115**, E4758–E4766 (2018).
103. Best, R. B., Zheng, W. & Mittal, J. Balanced protein-water interactions improve properties of disordered proteins and non-specific protein association. *J. Chem. Theory Comput.* **10**, 5113–5124 (2014).
104. Zhou, R. Replica exchange molecular dynamics method for protein folding simulation. *Methods Mol. Biol.* **350**, 205–223 (2007).
105. Schnapka, V. et al. Atomic resolution ensembles of intrinsically disordered proteins with Alphafold. *Nat Commun.* https://doi.org/10.1038/s41467-026-69172-y (2026).
106. Brotzakis, Z. F., Zhang, S., Murtada, M. H. & Vendruscolo, M. AlphaFold prediction of structural ensembles of disordered proteins. *Nat. Commun.* **16**, 1632 (2025).
107. Dignon, G. L., Zheng, W., Kim, Y. C., Best, R. B. & Mittal, J. Sequence determinants of protein phase behavior from a coarse-grained model. *PLoS Comput. Biol.* **14**, e1005941 (2018).
108. Tesei, G., Schulze, T. K., Crehuet, R. & Lindorff-Larsen, K. Accurate model of liquid-liquid phase behavior of intrinsically disordered proteins from optimization of single-chain properties. *Proc. Natl. Acad. Sci. USA* **118**, e2111696118 (2021).
109. Cao, F., von Bülow, S., Tesei, G. & Lindorff-Larsen, K. A coarse-grained model for disordered and multi-domain proteins. *Protein Sci.* **33**, e5172 (2024).
110. Chew, P. Y., Joseph, J. A., Collepardo-Guevara, R. & Reinhardt, A. Thermodynamic origins of two-component multiphase condensates of proteins. *Chem. Sci.* **14**, 1820–1836 (2023).
111. Emenecker, R. J., Guadalupe, K., Shamoon, N. M., Sukenik, S. & Holehouse, A. S. Sequence-ensemble-function relationships for disordered proteins in live cells. Preprint at *bioRxiv* https://doi.org/10.1101/2023.10.29.564547 (2023).
112. Pesce, F. et al. Design of intrinsically disordered protein variants with diverse structural properties. *Sci. Adv.* **10**, eadm9926 (2024).
113. Krueger, R.K., Brenner, M.P. & Shrinivas, K. Generalized design of sequence–ensemble–function relationships for intrinsically disordered proteins. *Nat. Comput. Sci.* https://doi.org/10.1038/s43588-025-00881-y (2025).

114. Harmon, T. S. et al. GADIS: algorithm for designing sequences to achieve target secondary structure profiles of intrinsically disordered proteins. *Protein Eng. Des. Sel.* **29**, 339–346 (2016).
115. Janson, G., Valdes-Garcia, G., Heo, L. & Feig, M. Direct generation of protein conformational ensembles via machine learning. *Nat. Commun.* **14**, 774 (2023).
116. Lewis, S. et al. Scalable emulation of protein equilibrium ensembles with generative deep learning. *Science* https://doi.org/10.1126/science.adv9817 (2025).
117. Janson, G. & Feig, M. Transferable deep generative modeling of intrinsically disordered protein conformations. *PLoS Comput. Biol.* **20**, e1012144 (2024).
118. Zhang, O. et al. Learning to evolve structural ensembles of unfolded and disordered proteins using experimental solution data. *J. Chem. Phys.* **158**, 174113 (2023).
119. Norgaard, A. B., Ferkinghoff-Borg, J. & Lindorff-Larsen, K. Experimental parameterization of an energy function for the simulation of unfolded proteins. *Biophys. J.* **94**, 182–192 (2008).
120. An, Y., Webb, M. A. & Jacobs, W. M. Active learning of the thermodynamics-dynamics trade-off in protein condensates. *Sci. Adv.* **10**, eadj2448 (2024).
121. von Bülow, S., Tesei, G., Zaidi, F. K., Mittag, T. & Lindorff-Larsen, K. Prediction of phase-separation propensities of disordered proteins from sequence. *Proc. Natl Acad. Sci. USA* **122**, e2417920122 (2025).
122. Bonomi, M., Heller, G. T., Camilloni, C. & Vendruscolo, M. Principles of protein structural ensemble determination. *Curr. Opin. Struct. Biol.* **42**, 106–116 (2017).
123. Stöckelmaier, J. & Oostenbrink, C. Combining simulations and experiments - a perspective on maximum entropy methods. *Phys. Chem. Chem. Phys.* **27**, 14704–14717 (2025).
124. Bottaro, S., Bengtsen, T. & Lindorff-Larsen, K. Integrating molecular simulation and experimental data: a bayesian/maximum entropy reweighting approach. *Methods Mol. Biol.* **2112**, 219–240 (2020).
125. Hummer, G. & Köfinger, J. Bayesian ensemble refinement by replica simulations and reweighting. *J. Chem. Phys.* **143**, 243150 (2015).
126. Bernadó, P., Mylonas, E., Petoukhov, M. V., Blackledge, M. & Svergun, D. I. Structural characterization of flexible proteins using small-angle X-ray scattering. *J. Am. Chem. Soc.* **129**, 5656–5664 (2007).
127. Nodet, G. et al. Quantitative description of backbone conformational sampling of unfolded proteins at amino acid resolution from NMR residual dipolar couplings. *J. Am. Chem. Soc.* **131**, 17908–17918 (2009).
128. Ferrie, J. J. & Petersson, E. J. A unified de novo approach for predicting the structures of ordered and disordered proteins. *J. Phys. Chem. B* **124**, 5538–5548 (2020).
129. Jussupow, A., Bartley, D., Lapidus, L. J. & Feig, M. COCOMO2: a coarse-grained model for interacting folded and disordered proteins. *J. Chem. Theory Comput.* **21**, 2095–2107 (2025).
130. Pesce, F. et al. Assessment of models for calculating the hydrodynamic radius of intrinsically disordered proteins. *Biophys. J.* **122**, 310–321 (2023).
131. Chodera, J. D. & Noé, F. Markov state models of biomolecular conformational dynamics. *Curr. Opin. Struct. Biol.* **25**, 135–144 (2014).
132. Mehdi, S., Smith, Z., Herron, L., Zou, Z. & Tiwary, P. Enhanced sampling with machine learning. *Annu. Rev. Phys. Chem.* **75**, 347–370 (2024).
133. Lindorff-Larsen, K. & Ferkinghoff-Borg, J. Similarity measures for protein ensembles. *PLoS ONE* **4**, e4203 (2009).
134. Lyle, N., Das, R. K. & Pappu, R. V. A quantitative measure for protein conformational heterogeneity. *J. Chem. Phys.* **139**, 121907 (2013).
135. Lazar, T. et al. Distance-based metrics for comparing conformational ensembles of intrinsically disordered proteins. *Biophys. J.* **118**, 2952–2965 (2020).
136. Aina, A., Hsueh, S. C. C. & Plotkin, S. S. PROTHON: a local order parameter-based method for efficient comparison of protein ensembles. *J. Chem. Inf. Model.* **63**, 3453–3461 (2023).
137. Ting, D. et al. Neighbor-dependent ramachandran probability distributions of amino acids developed from a hierarchical Dirichlet process model. *PLoS Comput. Biol.* **6**, e1000763 (2010).
138. González-Delgado, J. et al. WASCO: a Wasserstein-based statistical tool to compare conformational ensembles of intrinsically disordered proteins. *J. Mol. Biol.* **435**, 168053 (2023).
139. McClendon, C. L., Hua, L., Barreiro, A. & Jacobson, M. P. Comparing conformational ensembles using the Kullback-Leibler divergence expansion. *J. Chem. Theory Comput.* **8**, 2115–2126 (2012).
140. Scalvini, B. et al. Circuit topology approach for the comparative analysis of intrinsically disordered proteins. *J. Chem. Inf. Model.* **63**, 2586–2602 (2023).
141. Lotthammer, J. M. & Holehouse, A. S. Disentangling folding from energetic traps in simulations of disordered proteins. *J. Chem. Inf. Model.* **65**, 2897–2910 (2025).
142. Lotthammer, J. M., Ginell, G. M., Griffith, D., Emenecker, R. J. & Holehouse, A. S. Direct prediction of intrinsically disordered protein conformational properties from sequence. *Nat. Methods* **21**, 465–476 (2024).
143. Hofmann, H. et al. Polymer scaling laws of unfolded and intrinsically disordered proteins quantified with single-molecule spectroscopy. *Proc. Natl. Acad. Sci. USA* **109**, 16155–16160 (2012).
144. Holehouse, A. S., Das, R. K., Ahad, J. N., Richardson, M. O. G. & Pappu, R. V. CIDER: resources to analyze sequence-ensemble relationships of intrinsically disordered proteins. *Biophys. J.* **112**, 16–21 (2017).
145. Del Conte, A. et al. RING 4.0: faster residue interaction networks with novel interaction types across over 35,000 different chemical structures. *Nucleic Acids Res.* **52**, W306–W312 (2024).
146. González-Delgado, J., Bernadó, P., Neuvial, P. & Cortés, J. Weighted families of contact maps to characterize conformational ensembles of (highly-)flexible proteins. *Bioinformatics* **40**, btae627 (2024).
147. Thomasen, F. E. & Lindorff-Larsen, K. Conformational ensembles of intrinsically disordered proteins and flexible multidomain proteins. *Biochem. Soc. Trans.* **50**, 541–554 (2022).
148. Tompa, P. & Varadi, M. Predicting the predictive power of IDP ensembles. *Structure* **22**, 177–178 (2014).
149. Fuxreiter, M., Simon, I., Friedrich, P. & Tompa, P. Preformed structural elements feature in partner recognition by intrinsically unstructured proteins. *J. Mol. Biol.* **338**, 1015–1026 (2004).
150. Iconaru, L. I. et al. Discovery of small molecules that inhibit the disordered protein, $p27^{Kip1}$. *Sci. Rep.* **5**, 15686 (2015).
151. Basu, S. et al. Rational optimization of a transcription factor activation domain inhibitor. *Nat. Struct. Mol. Biol.* **30**, 1958–1969 (2023).
152. Chen, Q. -H. & Krishnan, V. V. Identification of ligand binding sites in intrinsically disordered proteins with a differential binding score. *Sci. Rep.* **11**, 22583 (2021).
153. Sciolino, N., Burz, D. S. & Shekhtman, A. In-cell NMR spectroscopy of intrinsically disordered proteins. *Proteomics* **19**, e1800055 (2019).
154. Moses, D. et al. Structural biases in disordered proteins are prevalent in the cell. *Nat. Struct. Mol. Biol.* **31**, 283–292 (2024).
155. Kryshtafovych, Schwede, A., Topf, T., Fidelis, M. & Moult, K. J. Critical assessment of methods of protein structure prediction (CASP)—Round XV. *Proteins* **91**, 1539–1549 (2023).

156. Mehdiabadi, M. et al. Critical assessment of protein intrinsic disorder round 3 - predicting disorder in the era of protein language models. *Proteins* 94, 414–424 (2026).
157. Cavender, C. E. et al. Structure-based experimental datasets for benchmarking protein simulation force fields. Preprint at https://arxiv.org/abs/2303.11056 (2025).
158. Svergun, D., Barberato, C. & Koch, M. H. J. CRYSOL – a program to evaluate X-ray solution scattering of biological macromolecules from atomic coordinates. *J. Appl. Crystallogr.* **28**, 768–773 (1995).
159. Trewhella, J. et al. A round-robin approach provides a detailed assessment of biomolecular small-angle scattering data reproducibility and yields consensus curves for benchmarking. *Acta Crystallogr. D Struct. Biol.* **78**, 1315–1336 (2022).
160. Hekstra, D. R. Emerging time-resolved X-ray diffraction approaches for protein dynamics. *Annu. Rev. Biophys.* **52**, 255–274 (2023).
161. Ragavan, M., Iconaru, L. I., Park, C. -G., Kriwacki, R. W. & Hilty, C. Real-time analysis of folding upon binding of a disordered protein by using dissolution DNP NMR spectroscopy. *Angew. Chem. Int. Ed. Engl.* **56**, 7070–7073 (2017).
162. Joshi, A. et al. Single-molecule FRET unmasks structural subpopulations and crucial molecular events during FUS low-complexity domain phase separation. *Nat. Commun.* **14**, 7331 (2023).
163. Seetaloo, N., Zacharopoulou, M., Stephens, A. D., Kaminski Schierle, G. S. & Phillips, J. J. Millisecond hydrogen/deuterium-exchange mass spectrometry approach to correlate local structure and aggregation in α-synuclein. *Anal. Chem.* **94**, 16711–16719 (2022).
164. Martin, E. W. et al. A multi-step nucleation process determines the kinetics of prion-like domain phase separation. *Nat. Commun.* **12**, 4513 (2021).
165. Le Ferrand, H., Duchamp, M., Gabryelczyk, B., Cai, H. & Miserez, A. Time-resolved observations of liquid-liquid phase separation at the nanoscale using in situ liquid transmission electron microscopy. *J. Am. Chem. Soc.* **141**, 7202–7210 (2019).
166. Kolloff, C. & Olsson, S. Rescuing off-equilibrium simulation data through dynamic experimental data with dynAMMo. *Mach. Learn. Sci. Technol.* **4**, 045050 (2023).
167. Ji, X., Wang, H. & Liu, W. Experiment-guided refinement of milestoning network. *J. Chem. Theory Comput.* **21**, 1078–1088 (2025).

Acknowledgements

This work was supported by: COST Action ML4NGP (CA21160), supported by COST (European Cooperation in Science and Technology); European Union through NextGenerationEU; PNRR project ELIXIRxNextGenIT (IR0000010); National Center for Gene Therapy and Drugs based on RNA Technology (CN00000041); European Union (101160233; HORIZON-Twinning project IDP2Biomed) and under grant agreement no. 101182949 (HORIZON-MSCA-SE project IDPfun2); Ministry of Education, Youth and Sport of the Czech Republic, within program Inter-Excellence II, INTER-COST (LUC23081); 2022.01454.PTDC (from The Foundation for Science and Technology (FCT), Portugal); Maria de Sousa Award 45/2022 (Bial Foundation and PT Medical Association); French National Research Agency (ANR) grants ANR-22-CE45-0003 and ANR-24-CE11-2382-03; NKFIH RGH_24 (RGH 151464); ItaliaDomani PNRR project 'Potentiating the Italian Capacity for Structural Biology Services in Instruct-ERIC' (ITACA.SB, no. IR0000009); and NKFIH RGH_24 (RGH 151464).

Views and opinions expressed are, however, those of the author(s) only and do not necessarily reflect those of the European Union or the European Research Executive Agency. Neither the European Union nor the granting authority can be held responsible for them.

Author contributions

All authors contributed to the discussion and the initial draft of this manuscript. H.G wrote the final document with the help of the co-authors. All authors edited and refined the final manuscript. A.M.M. and S.C.E.T. coordinated the project.

Competing interests

K.L.-L. holds stock options in and is a consultant for Peptone. All other authors declare no competing interests.

Additional information

Supplementary information The online version contains supplementary material available at https://doi.org/10.1038/s41592-026-03003-2.

Correspondence should be addressed to Silvio C. E. Tosatto or Alexander Miguel Monzon.

Peer review information *Nature Methods* thanks Anand Srivastava and the other, anonymous, reviewer(s) for their contribution to the peer review of this work.

Reprints and permissions information is available at www.nature.com/reprints.

Publisher's note Springer Nature remains neutral with regard to jurisdictional claims in published maps and institutional affiliations.

Springer Nature or its licensor (e.g. a society or other partner) holds exclusive rights to this article under a publishing agreement with the author(s) or other rightsholder(s); author self-archiving of the accepted manuscript version of this article is solely governed by the terms of such publishing agreement and applicable law.

© Springer Nature America, Inc. 2026

[1]Department of Biomedical Sciences, University of Padova, Padova, Italy. [2]Central European Institute of Technology (CEITEC), Masaryk University, Brno, Czech Republic. [3]National Centre for Biomolecular Research, Faculty of Science, Masaryk University, Brno, Czech Republic. [4]iBB—Institute for Bioengineering and Biosciences and and Department of Bioengineering, Instituto Superior Técnico, Universidade de Lisboa, Lisboa, Portugal. [5]Associate Laboratory i4HB—Institute for Health and Bioeconomy at Instituto Superior Técnico, Universidade de Lisboa, Lisboa, Portugal. [6]Centre de Biologie Structurale (CBS), Université de Montpellier, INSERM and CNRS, Montpellier, France. [7]LAAS-CNRS, Université de Toulouse, CNRS, Toulouse, France. [8]Department of Biochemistry, ELTE Eötvös Loránd University, Budapest, Hungary. [9]Department of Biochemistry and Molecular Biology, Michigan State University, East Lansing, MI, USA. [10]Structural Biology and NMR Laboratory, Linderstrøm-Lang Centre for Protein Science, Department of Biology, University of Copenhagen, Copenhagen, Denmark. [11]Johannes Kepler University, Institute of Biochemistry, Linz, Austria. [12]Department of Molecular Immunology and Toxicology and the National Tumor Biology Laboratory, National Institute of Oncology, Budapest, Hungary. [13]Department of Anatomy and Histology, HUN-REN–UVMB Laboratory of Redox Biology Research Group, University of Veterinary Medicine, Budapest, Hungary. [14]Chemistry Coordinating Institute, University of Debrecen, Debrecen, Hungary. [15]Semmelweis University, Budapest, Hungary. [16]Baruch S. Blumberg Institute, Doylestown, PA, USA. [17]The Wistar Institute, Philadelphia, PA, USA. [18]HUN-REN Office for Supported Research Groups (TKI), Cell Cycle Laboratory,

National Institute of Oncology, Budapest, Hungary. [19]Magnetic Resonance Center and Department of Chemistry "Ugo Schiff", University of Florence, Sesto Fiorentino, Florence, Italy. [20]Department of Biochemistry, University of Zurich, Zurich, Switzerland. [21]Department of Physics, University of Zurich, Zurich, Switzerland. [22]Centre de Biologie Structurale (CBS), CNRS - Univ. Montpellier - Inserm, Montpellier, France. [23]Institute of Molecular Life Sciences, HUN-REN Research Centre for Natural Sciences, Budapest, Hungary. [24]Yusuf Hamied Department of Chemistry, Centre for Misfolding Diseases, University of Cambridge, Cambridge, UK. [25]Institute of Organic Chemistry and Biochemistry, Czech Academy of Sciences, Prague, Czech Republic. [26]Structural Biology Brussels, Bio-engineering Department, Brussels, Belgium. [27]Interuniversity Institute of Bioinformatics in Brussels, Vrije Universiteit Brussel, Brussels, Belgium. [28]AI Lab, Vrije Universiteit Brussel, Brussels, Belgium. [29]Chemistry department, Vrije Universiteit Brussel, Brussels, Belgium. [30]Biomedical sciences, Vrije Universiteit Brussel, Brussels, Belgium. ✉e-mail: silvio.tosatto@unipd.it; alexander.monzon@unipd.it

nature methods

Supplementary information

https://doi.org/10.1038/s41592-026-03003-2

Toward a unified framework for determining conformational ensembles of disordered proteins

In the format provided by the authors and unedited

Supplementary Table 1: **Additional experimental techniques used to study IDP structural features**.

Summary of experimental methods that complement classical biophysical approaches for IDP analysis, including their forward models, information content, level of structural resolution, and system applicability (e.g., in vitro vs. in cell).

Technique	Experimental measurement	Forward Models / Computational tools / Theoretical models	Information content	Structural interpretation (e.g. residue level vs. global)	System perturbation	Environment (In-vivo / in-vitro / in-cell)	Reference database
Neutron Spin Echo (NSE) spectroscopy	Intermediate scattering function	Diffusion models	Provides dynamic information on nanosecond to microsecond timescales	Internal dynamics and diffusion	None required	In-vitro	N/A
Hydrogen deuterium exchange mass spectrometry (HDX-MS)	Kinetics of isotope substitution	Under development; HDXsimulator	Rate of proton/deuterium exchange	Exposure to the solvent, local stability, hydrogen bond formation	Gas phase, heavy water, back exchange	In-vitro / in-cell	Under development; ProteomeXchange
Circular dichroism (CD) spectroscopy	Differential absorption of left and right circularly polarized light	Secondary structure prediction algorithms	Provides secondary structure content	Secondary structure content	None required	In-vitro	PCDDB
Fluorescence anisotropy	Anisotropy	Perrin equation or molecular simulation	Local flexibility, rotational motion	Rotational correlation time	Dye labeling	In-vitro/in-cell	N/A
Fluorescence Correlation Spectroscopy (FCS)	Fluorescence intensity correlation	Stokes-Einstein or Stokes-Einstein-Debye	Rotational and translational motion	Hydrodynamic radius	Dye labeling	in -vitro/in-cell	N/A
Fourier Transform Infrared Spectroscopy (FTIR)	Infrared absorption spectrum	Vibrational modes analysis	Provides information on secondary structure and chemical bonds	Secondary structure, functional groups	None required	In-vitro	N/A
Limited Proteolysis coupled to Mass Spectrometry (LiP-MS)	Proteolytic cleavage patterns analyzed by mass spectrometry	Protease cleavage patterns and MS-detectable peptides	Provides insights into protein structure and conformational changes	Protein conformation and dynamics	Protease treatment	In-vitro	N/A
Dynamic light scattering (DLS)	Intensity fluctuations of scattered light	Stokes-Einstein equation	Provides size distribution of particles in solution	Hydrodynamic radius	None required	In-vitro	N/A
Cryogenic Electron Microscopy (CryoEM)	Electron scattering images	Electron density map modelling	Provides near-atomic resolution structures	High-resolution structures	Non required	In-vitro (frozen-hydrated samples)	EMDB
Laser-THz Emission Microscope (LTEM)	Electron scattering images	THz emission modelling	Similar to CryoEM	High-resolution structures	Non required	In-vitro (cryogenic temperatures)	N/A
Electron Paramagnetic Resonance (EPR)	Absorption of microwave radiation by unpaired electrons	Spin Hamiltonian analysis	Distance distributions, local dynamics	Local environment of unpaired electrons	Spin labeling	In-vitro/in-cell	N/A
Atomic Force Microscopy (AFM)	Force-distance curves	Force spectroscopy models	Provides high-resolution surface images and mechanical properties	Surface topography at the nanoscale	None required	In-vitro	N/A
Mass Spectrometry (MS)	Thermal Proteome Profiling (TPP)	Thermal stability profiles	Provides information on protein stability and interactions	Protein stability and folding states	Temperature changes	In vivo	N/A

Supplementary Table 2. Summary of conformational ensemble generation techniques. Classification of computational strategies for conformational ensemble generation based on the underlying modeling paradigm (knowledge-based, physics-based, machine learning, or hybrid), with evaluation of their strengths, limitations, and suitable applications.

Ensemble Generation Strategy	Method/ Force field	Core Principle	When to use	Strength	Limitation
Knowledge-based	Flexible Meccano[1]	Random coil-based sampling of backbone dihedrals using statistical distributions	When fast, generic IDP ensembles are needed without added data	Fast; simple; minimal input	No statistical weights; lacks side chains and atomistic detail
	TraDES[2]	Generates ensembles via statistical coil models and steric filtering	For baseline comparisons or when no structural data is available	Very efficient; customizable chain properties	No statistical weights; lacks experimental integration
	MoMA[3]	Builds conformers using motion planning algorithms with steric constraints and possibly incorporating energy models	When large-scale exploration with realistic geometry is desired	Includes full-atom models; physically plausible structures	Dynamics are not considered
	IDPConformerGenerator[4]	Samples torsion angles from fragment libraries, optionally guided by restraints	When integrating sequence and experimental restraints	Modular; supports reweighting and SAXS/NMR constraints	Depends on fragment quality and scoring functions
	RANCH[5]	Stochastic generation of flexible linkers and IDRs between rigid bodies, based on geometric constraints	When modeling large-scale flexibility or preparing SAXS ensembles	Very efficient; compatible with SAXS; minimal input required	No statistical weights; lacks atomistic detail; not suitable for local structure prediction
	DIPEND[6]	Generates ensembles using neighbor-dependent statistical dihedral angle distributions and structural filters	When fast backbone ensemble generation is needed from sequence with minimal input	Efficient and customizable; uses experimental priors; fast clash resolution and refinement steps	Lacks physical dynamics; relies on heuristics and rotamer libraries; limited to backbone sampling
Physics-based	Amber ff99SBws/ff03ws[7]	All-atom force field with improved water–protein interactions	For simulations of IDPs with balanced protein-water interactions	Improved global dimensions and protein-protein association	Computationally intensive
	Amber f99SB-disp[8]	Dispersion-corrected all-atom force field for IDPs and folded proteins	For simulations of IDPs and folded proteins	Improved global dimensions and transient helicity	Computationally intensive
	DES-Amber[9]	All-atom force field with improved description of protein-protein complexes	For simulations of IDPs, folded proteins, and protein-protein complexes	Improved global dimensions, transient helicity, and protein-protein complexes	Limited to Amber ecosystem
	REMD[10]	Parallel simulations at different temperatures for enhanced sampling	To improve conformational sampling in rugged energy landscapes	Better sampling of rare conformers	Requires many replicas; costly
	Metadynamics[11]	Biases applied to accelerate rare event sampling	When slow transitions hinder sampling of	Efficient barrier crossing	Choice of the collective variables may affect efficiency

			conformers		
	ABSINTH[12]	Implicit-solvent all-atom force field for IDPs	Fast all-atom modeling of long IDPs	Efficient; all-atom resolution	Lacks explicit solvent detail
	MARTINI[13]	Widely used coarse-grained model for large biomolecular systems	For large-scale or membrane-associated systems	Scalable to large complexes	Simplified interactions
	Mpipi[14]	Implicit-solvent coarse-grained force field for IDPs; bottom-up and top-down parameterization	Fast and sequence-dependent modeling of IDPs	Efficient; accurate predictions of IDP compaction	Residue-level resolution; does not capture transient secondary structure or hydrogen bonding
	CALVADOS[15,16]	Implicit-solvent coarse-grained force field for IDPs and multi-domain proteins; top-down parameterization.	Fast and sequence-dependent modeling of IDPs and multi-domain proteins	Efficient; accurate predictions of IDP compaction	Residue-level resolution; does not capture transient secondary structure or hydrogen bonding
	HPS[17]	Implicit-solvent coarse-grained force field for IDPs and multi-domain proteins; bottom-up parameterization	Fast and sequence-dependent modeling of IDPs	Efficient; captures trends in IDP compaction	Residue-level resolution; does not capture transient secondary structure or hydrogen bonding; may overestimate IDP compaction
Machine-Learning	idpGAN[18]	GAN trained on CG-MD generated ensembles to generate new conformers with statistical characteristics of training data	When need rapid ensemble generation	Captures realistic ensemble diversity; scalable	Limited to patterns learned; learns fromCG training data; Cα-only ensembles
	idpSAM[19]	Latent diffusion model (transformer autoencoder + diffusion) trained on implicit-solvent ensembles (ABSINTH) to sample new structures	For generating ensembles of short IDRs (< 60 residues), transfers to sequences absent in training set	High generalization to unseen sequences; stable training	Requires substantial training data from simulations
	STARLING[20]	Diffusion/generative approach leveraging physics-based insights to produce hundreds of conformers in seconds	When needing rapid, large-scale ensemble predictions from sequence	Extremely fast (< seconds); works on both GPU & CPU	Newer tool; may lack extensive validation across diverse sequences
	IDPFold[21]	Fine-tuned diffusion model generating backbone-level conformers directly from sequence, without MSAs or experimental input	When backbone ensemble prediction is needed rapidly from sequence alone	Bypasses need for MSA or experiments; provides diverse structural features	Focuses on backbone only; may miss side-chain dynamics and solvent effects
	Phanto-IDP[22]	Diffusion-based generative model trained on sequence-conditioned structural features of IDPs	When rapid ensemble generation is needed from sequence alone	Physics-informed generative model; captures IDP-specific features; fast sampling	Relies on training data quality; may lack fine-resolution structural detail
	BioEmu[23]	Diffusion model trained on a large dataset of simulation and experimental data	Rapid generation of equilibrium ensembles from sequence	Fast and sequence-sensitive; produces diverse ensembles consistent with disordered behavior	Backbone-only, lacks sidechain sampling;; overestimates radius of gyration for longer IDPs (>100

					residues)
Hybrid	AlphaFold-Metainference[24]	Combines AlphaFold constraints with Bayesian ensemble modeling (ML + Physics-based approach)	To integrate AI predictions into ensemble refinement	Incorporates prior knowledge	Requires AlphaFold confidence and priors
	FastFloppyTail [25]	Uses Rosetta fragment insertion with modified energy terms and sampling strategies optimized for IDPs(Physics-based + knowledge-based)	For IDPs requiring backbone ensembles with local structure propensity	Combines knowledge-based fragment sampling with physics-informed scoring; accurate for local motifs	Computationally intensive; coarse side-chain modeling; limited by fragment library quality
	DynamICE[26]	Uses a Generative Recurrent Neural Network (GRNN) to generate conformers, fine-tune with experimental data via a Bayesian reward function (X-EISD). (ML + ME)	When fixed pools are insufficient and data-driven generation of diverse IDP ensembles is needed.	Enables de novo, data-consistent conformer generation, integrates physical and experimental constraints, and improves iteratively.	Torsion-based (local) sampling makes it suboptimal to accurately satisfy distance restraints like NOEs and PREs.
	AF2-RAVE[27]	Combines AlphaFold2 (with reduced MSA) + short MD + machine learning (SPIB)	When diverse functional states are needed from sequence with minimal prior knowledge	Efficiently maps conformational landscape; captures metastable states; integrates physical and statistical modeling	Requires short MD; not suitable for ultra-fast motions; moderate compute setup needed
	bAles[28]	Bayesian integration of AlphaFold2 distograms as distance restraints into a random coil model as a prior	For generating atomistic IDP ensembles efficiently, especially when experimental data is limited	Fast; atomistic resolution; robust to AF2 errors; captures local & long-range features	Dependent on AF2 accuracy; limited for environment-sensitive or transient contacts
	AFflecto[29]	Builds IDP ensembles using fragment-based sampling informed by AlphaFold models, with secondary structure element(SSE) and steric constraints	When needing efficient conformer generation guided by AlphaFold predictions and optional SSE control	Fast and tunable; incorporates partial structure; no MD or force fields required	No dynamic sampling; side chains approximated with pseudo atoms

Supplementary Table 3. Experimental data integration techniques for conformational ensemble refinement.
Comparison of methods used to integrate experimental data (e.g., SAXS, NMR, smFRET) into structural ensemble modeling. Integration strategies include maximum entropy, maximum parsimony, and hybrid approaches, along with their assumptions and computational features.

Integration Strategy	Method	Core Principle	When to use	Strength	Limitation
Maximum Entropy	X-EISD[30]	Bayesian inference using error models to compare ensembles to various experimental data	When integrating NMR/SAXS data with structural ensembles	Handles multiple data types; includes uncertainty; enables reweighting	Needs accurate error models; relies on ensemble diversity
	EROS[31]	Maximum-entropy reweighting of simulation ensemble to fit SAXS data	Flexible or disordered proteins with SAXS data and simulated ensembles	Avoids overfitting	Computationally demanding
	BioEn[32]	Combines EROS with simulations and reweighting to refine ensembles	When you want accurate ensemble refinement with control over data vs. model balance	Faster convergence; explores multiple confidence levels (θ) without extra simulations	More complex setup; depends on good sampling and reweighting
	COPER[33]	Uses convex optimization to reweight large ensembles to fit experimental averages	When working with very large ensembles and average experimental observables (e.g., SAXS, NMR)	Highly efficient and scalable; guarantees convergence and stability	Does *not* offer uncertainty estimates for the reweighted ensemble weights, unlike Bayesian approaches.
	BME[34]	Bayesian/maximum-entropy reweighting of ensembles using experimental averages with uncertainty	When combining simulations with experimental data (e.g., NMR, SAXS)	Accounts for data uncertainty; balances fit and prior; reusable weights	Requires tuning; depends on ensemble quality
	BEGR[35]	Reweights ensembles to match residue-level secondary structure content from chemical shifts	When experimental NMR chemical shifts are available and you aim to refine an existing IDP ensemble to achieve accurate secondary structure distributions	Achieves converged ensemble distributions; directly uses experimental constraints	Depends on quality of initial ensemble and secondary structure predictions from chemical shifts
	Metainference[36]	Simultaneously infers structural ensembles and experimental errors by integrating prior distributions and data uncertainty into a Bayesian framework.	Best suited for heterogeneous systems (e.g., IDPs, multi-state folded proteins) and when data noise and structural variability must be jointly modeled.	Metainference rigorously accounts for experimental noise, ensemble heterogeneity, and uncertainty in observables, uses a replica-averaged likelihood, and is integrated with molecular dynamics (e.g., PLUMED) to sample ensembles	Computationally demanding, requires integration with MD simulations, and may be complex for users unfamiliar with Bayesian inference.

				on-the-fly.	
	ENSEMBLE[37]	Adjusts weights on a pool of conformers to match experimental data while preserving ensemble diversity	When analyzing IDPs with diverse experimental restraints requiring a flexible, data-consistent ensemble	ENSEMBLE supports a wide range of experimental data types, allows flexible weighting of both conformers and data modules, preserves ensemble diversity, and integrates with external tools for accurate back-calculation.	It requires a large, pre-generated conformer pool, can be computationally intensive for large datasets, and offers lower interpretability due to the complexity of weighted ensembles.
Maximum Parsimony	EOM[5]	Selects a small subset of conformers from a large random pool to best fit SAXS data, using a genetic algorithm.	When interpreting SAXS data for disordered or flexible proteins, especially when interested in overall shape and size distributions.	EOM is tailored for SAXS analysis, offers intuitive control over ensemble size and fit quality, produces interpretable distributions (e.g., Rg, Dmax), and is fast and easy to use for flexibility profiling.	It supports only SAXS data, relies on pre-generated conformers, and may oversimplify underlying structural heterogeneity due to its reliance on a small subset.
	ASTEROIDS[38]	Uses a genetic algorithm to select a fixed-size ensemble of conformers from a large pool that minimizes deviation from experimental data using a multi-component fitness function.	When you need a sparse, interpretable ensemble that fits RDCs, PREs, or NOEs, and want robust, global optimization of ensemble composition.	ASTEROIDS builds minimal ensembles with strong data agreement, uses explicit fitness weighting by data type, and employs genetic diversity mechanisms (mutation, crossover, tournaments) to avoid local minima and improve robustness across 2000+ generations.	It requires a fixed conformational collection size, lacks conformer weighting (binary inclusion only), may underrepresent structural diversity, and is tailored mainly for NMR restraints, limiting applicability to multimodal datasets.
	SES[39]	Selects the sparsest possible weighted ensemble from an oversampled conformer pool that fits experimental data within a defined error, using deterministic optimization.	Ideal for systems with underdetermined experimental data (e.g., RDCs, SAXS) where sparse conformational representation is desired and data scaling is uncertain.	SES provides a deterministic and scalable algorithm (Multi-OMP), avoids overfitting via rigorous -curve analysis, recovers robust ensemble weights, and requires no prior assumptions about weight distributions.	Requires an accurate prediction model for experimental observables, depends on quality and coverage of the input conformer pool, and currently supports only linearly averaged data (e.g., RDCs, SAXS).
Other	MMMx[40]	Reweights precomputed conformer ensembles to match experimental data (e.g., DEER, SAXS) via non-negative least squares or Monte Carlo sampling	When refining large conformer pools with multi-modal experimental restraints	Handles diverse data types; supports block-wise fitting and pruning; efficient for large ensembles	Reweighting can bias ensemble toward overrepresented states if prior is poor

Supplementary Table 4. Summary of conformational ensemble comparison techniques. Summary of methods and metrics for quantifying similarities and differences between conformational ensembles. Includes descriptor-based, probabilistic, topological, and energy-based approaches, with notes on their computational complexity and interpretability.

Method/Metric	Description	Advantages	Disadvantages	Computational cost
Conformational Heterogeneity[41]	Computes inter-residue distances across ensemble conformers to yield a single scalar quantifying conformational diversity.	Simple to implement; provides a quick overview of ensemble heterogeneity.	Overly simplistic; fails to capture local or multimodal structural differences.	Low
Residue Pair Distance Matrices[42]	Compares conformational ensembles via statistical analysis of residue–residue distance matrices.	Easy to compute and to interpret.	Comparisons based on median and standard deviation of distances, but not on the distribution of values..	Moderate
Kullback-Leibler (KL) or Jensen-Shannon (JS) Divergence based on Probability Density Estimates[43,44]	Estimates the probability density of a conformational space descriptor and quantifies the difference between ensembles based on KL or JS divergence.	Considers relevant descriptors of conformational variability.	Precise estimation of probability density is a challenge for highly dynamic systems.	Moderate to high
Wasserstein Distance Considering Local and Global Descriptors[45]	It computes the "cost" of transforming one ensemble distribution into another, using local descriptors (backbone angle distributions for each residue) and global descriptors (inter-residue distances).	Provides intuitive interpretation as "minimum effort" to morph one ensemble into another; robust to outliers; identifies the residues/regions that contribute most significantly; alignment-free.	Computationally intensive; scaling to large ensembles or high-dimensional descriptors can be demanding.	High
Topology-Based Metrics[46]	Compares ensembles by analyzing differences in contact-based graph topology.	Captures global rearrangements; alignment-free.	Lacks geometric detail; may oversimplify structure.	Moderate
Local Energy Trap Analysis [47]	Identifies residues with persistent low-energy conformers across ensemble	Highlights energetic hotspots; links sequence to ensemble behavior	Force field-dependent; may require good sampling	Moderate

Supplementary Table 5. Proposed Scoring Metrics and Evaluation Criteria for IDP-Bench Submissions

Experimental Technique	Scoring metric	Structural Resolution	Advantages	Limitations
SAXS	X^2 score between full SAXS profiles (I(q) vs q) of experimental and computed ensemble; residual analysis	Global	Sensitive to overall dimensions and shape; fast and widely available	Low resolution; ensemble averaging; hydration layer and buffer condition effects
smFRET	Wasserstein distance between predicted and measured distance distributions	Local & Global	Reports on full distance distributions; resolves subpopulations	Requires careful control of dye labeling, orientation, and mobility
RDCs	Q-factor	Local	Sensitive to bond vector orientations and secondary structure propensities	May requires alignment tensors; sensitive to artifacts from alignment media
PRE	RMSE of PRE intensities	Local	Captures long-range transient contacts; informative for compactness	Sensitive to spin-label flexibility; forward model uncertainties
Chemical Shifts	RMSE or correlation coefficients	Local	Standardized and broadly available; reflects secondary structure propensity	Sensitive to sequence context and environmental effects
HDX-MS	Protection factor deviation	Local(per-segment)	Reports on transient structural protection; complementary to NMR	Resolution depends on peptide coverage; requires careful experimental setup
Hydrodynamic radius(e.g. from DOSY)	ΔR_h from predicted vs. measured	Global	Fast readout of chain compaction/expansion	Influenced by buffer viscosity, temperature, and shape assumptions

Supplementary Figure 1: Overview of the IDP-Bench benchmarking framework. The four-phase cycle includes data curation, blind ensemble prediction, multi-modal scoring, and public dissemination. Evaluation incorporates diverse experimental inputs and standardized metrics to assess global and local ensemble accuracy. Created in BioRender. Ghafouri, H. (2025) https://BioRender.com/i36we79.

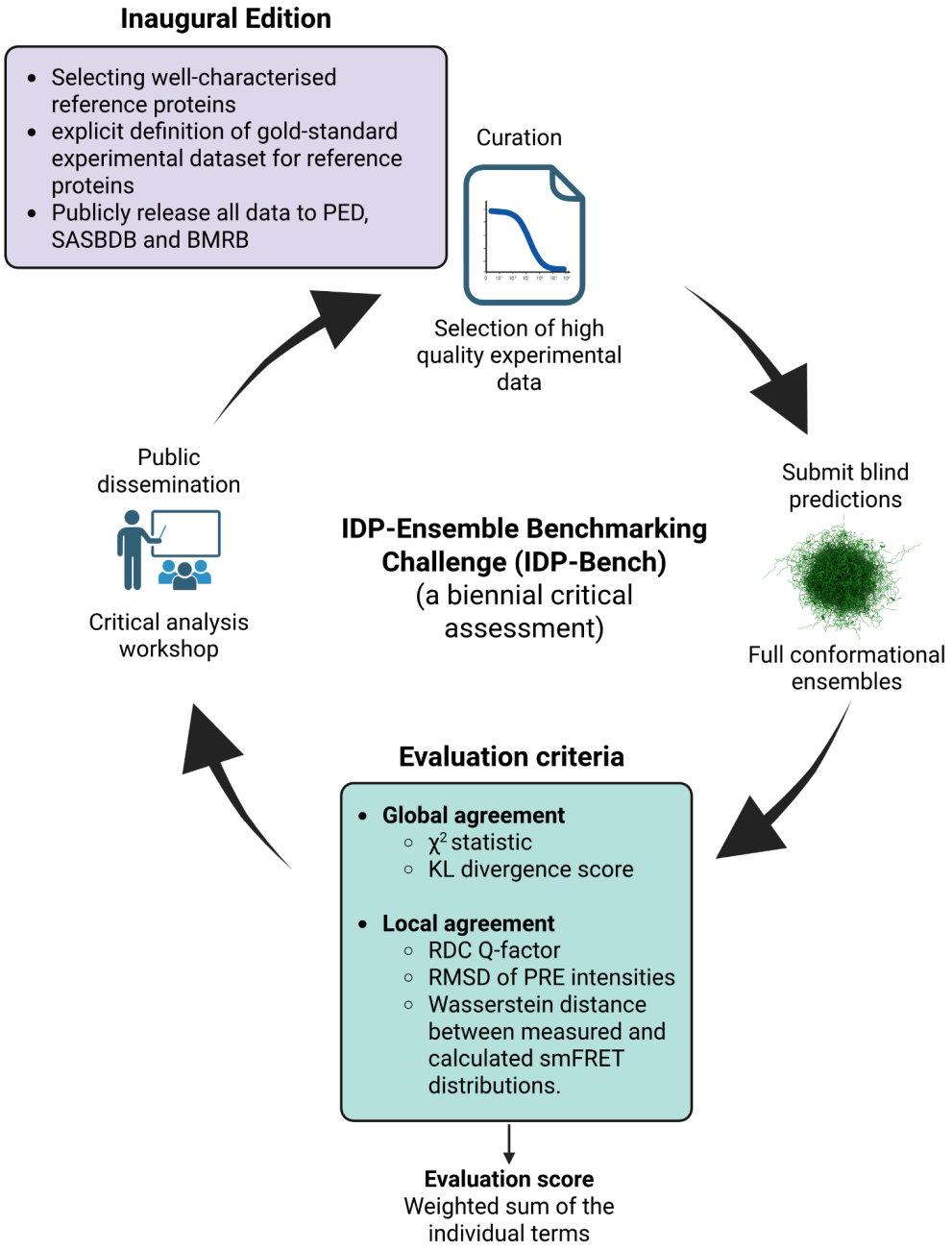

Supplementary Figure 2. Error landscape in integrative ensemble determination of intrinsically disordered proteins (IDPs) using NMR, smFRET, and SAXS. The schematic summarizes typical experimental and modeling uncertainties associated with each method. **NMR:** Chemical shift uncertainties range from ±0.02 ppm (^{1}H) to ±0.35 ppm for ^{13}C/^{15}N, though systematic referencing errors are often dominant. J-coupling and RDC errors are ~0.5 Hz; relaxation rates are typically underdetermined and often assigned an arbitrary error (~3%). For chemical shifts, experimental errors are much smaller than predictor errors. Forward models for chemical shift mainly have standard deviations of 1.0 ppm for backbone Cα predictions on their training datasets[48]. **smFRET:** FRET efficiency measurements have inter-lab standard deviations of ±0.02 to ±0.05, systematic error dominated by instrument calibration (corresponding distance uncertainties are ±2–3 Å) and the uncertainty in the Förster radius (R_0), which has been estimated to be ~7%[49]. In sm-FRET forward models based on rotamer libraries, a source of uncertainty is the assumption about the timescales of linker and dye motions[50]. For FRETpredict[51], this uncertainty can affect the predicted FRET efficiency up to ~15%. **SAXS:** Radius of gyration (Rg) is the most reliable parameter, with <1.5 Å uncertainty for folded proteins (slightly higher for large Rg proteins)[52]. Molecular weight (MW) determination from scattering intensity has ~10% error, while maximum dimension (Dmax) is poorly defined for IDPs and typically underestimates the true value by 10–15%. Systematic errors in SAXS forward models stem largely from solvent treatment and vary with protein features. Created in BioRender. Ghafouri, H. (2025) https://BioRender.com/c2irt8f

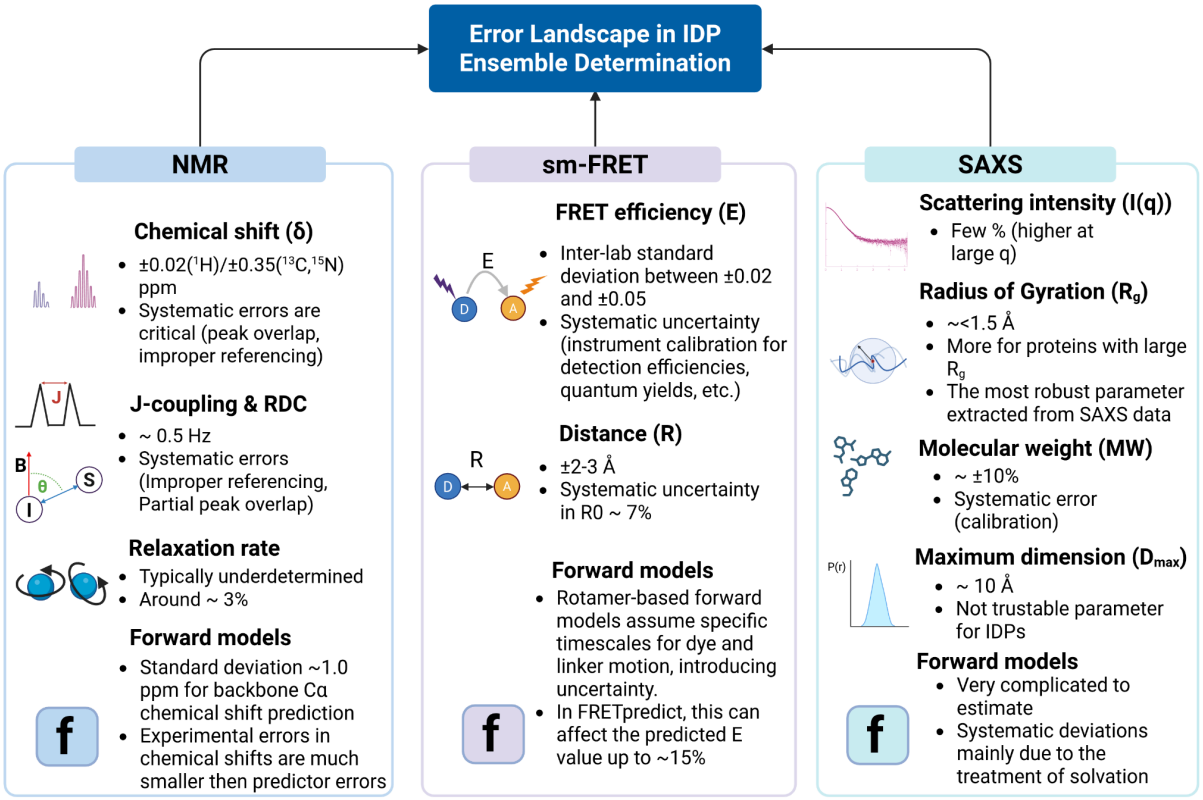

Supplementary Figure 3. Decision diagram for IDP conformational ensemble determination. A conceptual workflow diagram highlighting key decision points in the selection of computational and experimental strategies for generating and refining structural ensembles of IDPs.

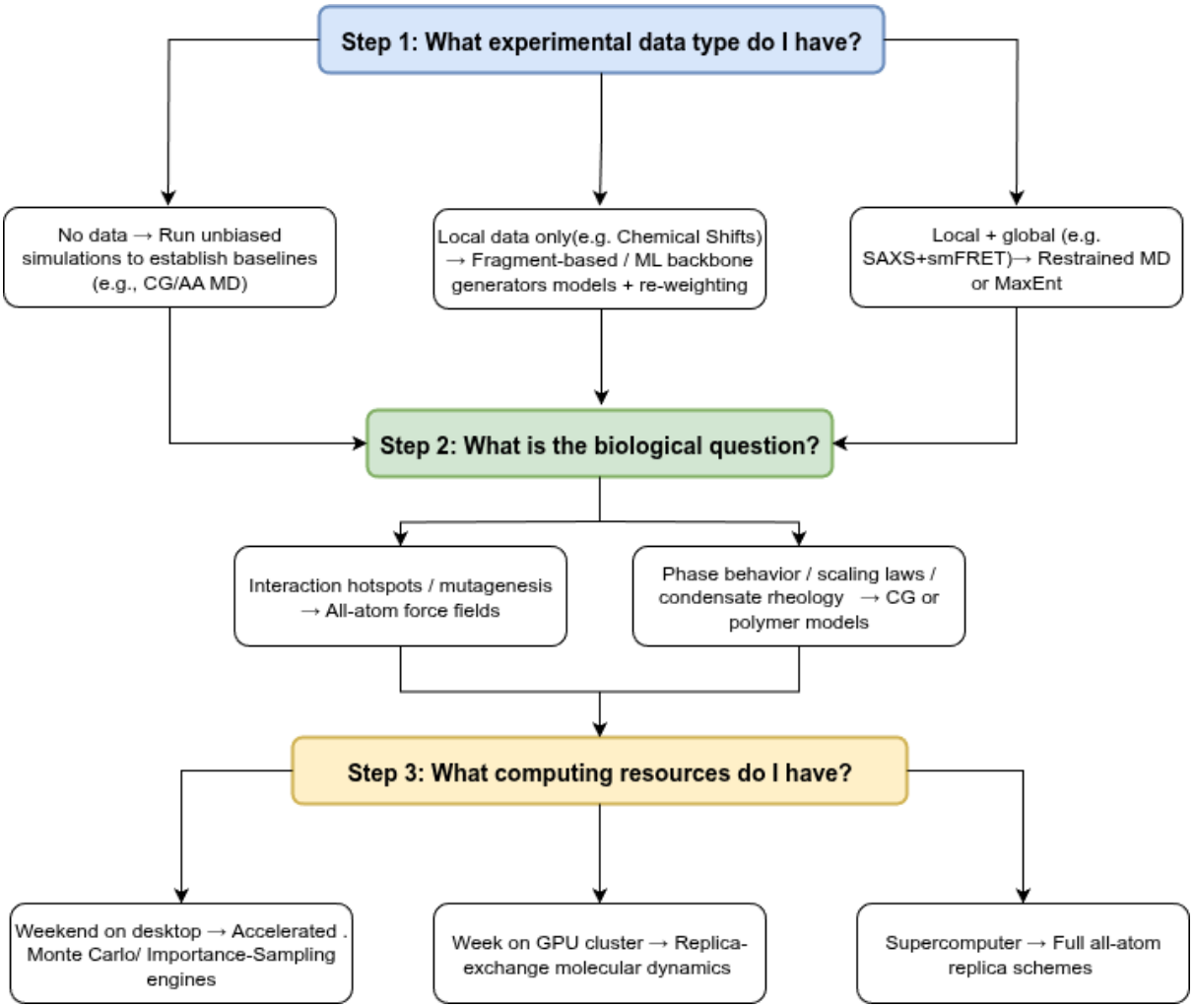

Supplementary References

1. Ozenne, V. *et al.* Flexible-meccano: a tool for the generation of explicit ensemble descriptions of intrinsically disordered proteins and their associated experimental observables. *Bioinforma. Oxf. Engl.* **28**, 1463–1470 (2012).
2. Feldman, H. J. & Hogue, C. W. V. Probabilistic sampling of protein conformations: New hope for brute force? *Proteins Struct. Funct. Bioinforma.* **46**, 8–23 (2002).
3. Barozet, A. *et al.* MoMA-LoopSampler: a web server to exhaustively sample protein loop conformations. *Bioinformatics* **38**, 552–553 (2022).
4. Teixeira, J. M. C. *et al.* IDPConformerGenerator: A Flexible Software Suite for Sampling the Conformational Space of Disordered Protein States. *J. Phys. Chem. A* **126**, 5985–6003 (2022).
5. Bernadó, P., Mylonas, E., Petoukhov, M. V., Blackledge, M. & Svergun, D. I. Structural characterization of flexible proteins using small-angle X-ray scattering. *J. Am. Chem. Soc.* **129**, 5656–5664 (2007).
6. Harmat, Z., Dudola, D. & Gáspári, Z. DIPEND: An Open-Source Pipeline to Generate Ensembles of Disordered Segments Using Neighbor-Dependent Backbone Preferences. *Biomolecules* **11**, 1505 (2021).
7. Best, R. B., Zheng, W. & Mittal, J. Balanced Protein-Water Interactions Improve Properties of Disordered Proteins and Non-Specific Protein Association. *J. Chem. Theory Comput.* **10**, 5113–5124 (2014).
8. Robustelli, P., Piana, S. & Shaw, D. E. Developing a molecular dynamics force field for both folded and disordered protein states. *Proc. Natl. Acad. Sci. U. S. A.* **115**, E4758–E4766 (2018).
9. Piana, S., Robustelli, P., Tan, D., Chen, S. & Shaw, D. E. Development of a Force Field for the Simulation of Single-Chain Proteins and Protein–Protein Complexes. *J. Chem. Theory Comput.* **16**, 2494–2507 (2020).
10. Zhou, R. Replica exchange molecular dynamics method for protein folding simulation. *Methods Mol. Biol. Clifton NJ* **350**, 205–223 (2007).
11. Bonomi, M., Barducci, A. & Parrinello, M. Reconstructing the equilibrium Boltzmann distribution from well-tempered metadynamics. *J. Comput. Chem.* **30**, 1615–1621 (2009).
12. Vitalis, A. & Pappu, R. V. ABSINTH: A new continuum solvation model for simulations

of polypeptides in aqueous solutions. *J. Comput. Chem.* **30**, 673–699 (2009).

13. Souza, P. C. T. *et al.* Martini 3: a general purpose force field for coarse-grained molecular dynamics. *Nat. Methods* **18**, 382–388 (2021).

14. Joseph, J. A. *et al.* Physics-driven coarse-grained model for biomolecular phase separation with near-quantitative accuracy. *Nat. Comput. Sci.* **1**, 732–743 (2021).

15. Tesei, G., Schulze, T. K., Crehuet, R. & Lindorff-Larsen, K. Accurate model of liquid-liquid phase behavior of intrinsically disordered proteins from optimization of single-chain properties. *Proc. Natl. Acad. Sci. U. S. A.* **118**, e2111696118 (2021).

16. Cao, F., von Bülow, S., Tesei, G. & Lindorff-Larsen, K. A coarse-grained model for disordered and multi-domain proteins. *Protein Sci. Publ. Protein Soc.* **33**, e5172 (2024).

17. Dignon, G. L., Zheng, W., Kim, Y. C., Best, R. B. & Mittal, J. Sequence determinants of protein phase behavior from a coarse-grained model. *PLoS Comput. Biol.* **14**, e1005941 (2018).

18. Janson, G., Valdes-Garcia, G., Heo, L. & Feig, M. Direct generation of protein conformational ensembles via machine learning. *Nat. Commun.* **14**, 774 (2023).

19. Janson, G. & Feig, M. Transferable deep generative modeling of intrinsically disordered protein conformations. *PLOS Comput. Biol.* **20**, e1012144 (2024).

20. Novak, B., Lotthammer, J. M., Emenecker, R. J. & Holehouse, A. S. Accurate predictions of conformational ensembles of disordered proteins with STARLING. 2025.02.14.638373 Preprint at https://doi.org/10.1101/2025.02.14.638373 (2025).

21. Zhu, J. *et al.* Precise Generation of Conformational Ensembles for Intrinsically Disordered Proteins via Fine-tuned Diffusion Models. 2024.05.05.592611 Preprint at https://doi.org/10.1101/2024.05.05.592611 (2024).

22. Zhu, J. *et al.* Phanto-IDP: compact model for precise intrinsically disordered protein backbone generation and enhanced sampling. *Brief. Bioinform.* **25**, bbad429 (2024).

23. Lewis, S. *et al.* Scalable emulation of protein equilibrium ensembles with generative deep learning. *Science* eadv9817 (2025).

24. Brotzakis, Z. F., Zhang, S., Murtada, M. H. & Vendruscolo, M. AlphaFold prediction of structural ensembles of disordered proteins. *Nat. Commun.* **16**, 1632 (2025).

25. Ferrie, J. J. & Petersson, E. J. A Unified De Novo Approach for Predicting the Structures of Ordered and Disordered Proteins. *J. Phys. Chem. B* **124**, 5538–5548 (2020).

26. Zhang, O. *et al.* Learning to evolve structural ensembles of unfolded and disordered proteins using experimental solution data. *J. Chem. Phys.* **158**, 174113 (2023).

27. Teng, D., Meraz, V. J., Aranganathan, A., Gu, X. & Tiwary, P. af2rave: protein ensemble generation with physics-based sampling. *Digit. Discov.* (2025).

28. Schnapka, V., Morozova, T., Sen, S. & Bonomi, M. Atomic resolution ensembles of intrinsically disordered and multi-domain proteins with Alphafold. 2025.06.18.660298 Preprint at https://doi.org/10.1101/2025.06.18.660298 (2025).

29. Pajkos, M., Clerc, I., Zanon, C., Bernadó, P. & Cortés, J. AFflecto: A web server to generate conformational ensembles of flexible proteins from AlphaFold models. *J. Mol. Biol.* 169003 (2025).

30. Lincoff, J. *et al.* Extended experimental inferential structure determination method in determining the structural ensembles of disordered protein states. *Commun. Chem.* **3**, 1–12 (2020).

31. Różycki, B., Kim, Y. C. & Hummer, G. SAXS ensemble refinement of ESCRT-III CHMP3 conformational transitions. *Struct. Lond. Engl. 1993* **19**, 109–116 (2011).

32. Hummer, G. & Köfinger, J. Bayesian ensemble refinement by replica simulations and reweighting. *J. Chem. Phys.* **143**, 243150 (2015).

33. Leung, H. T. A. *et al.* A Rigorous and Efficient Method To Reweight Very Large Conformational Ensembles Using Average Experimental Data and To Determine Their Relative Information Content. *J. Chem. Theory Comput.* **12**, 383–394 (2016).

34. Bottaro, S., Bengtsen, T. & Lindorff-Larsen, K. Integrating Molecular Simulation and Experimental Data: A Bayesian/Maximum Entropy Reweighting Approach. *Methods Mol. Biol. Clifton NJ* **2112**, 219–240 (2020).

35. Ytreberg, F. M., Borcherds, W., Wu, H. & Daughdrill, G. W. Using chemical shifts to generate structural ensembles for intrinsically disordered proteins with converged distributions of secondary structure. *Intrinsically Disord. Proteins* **3**, e984565 (2015).

36. Bonomi, M., Camilloni, C., Cavalli, A. & Vendruscolo, M. Metainference: A Bayesian inference method for heterogeneous systems. *Sci. Adv.* **2**, e1501177 (2016).

37. Choy, W. Y. & Forman-Kay, J. D. Calculation of ensembles of structures representing the unfolded state of an SH3 domain. *J. Mol. Biol.* **308**, 1011–1032 (2001).

38. Nodet, G. *et al.* Quantitative Description of Backbone Conformational Sampling of Unfolded Proteins at Amino Acid Resolution from NMR Residual Dipolar Couplings. *J.*

Am. Chem. Soc. **131**, 17908–17918 (2009).

39. Berlin, K. *et al.* Recovering a representative conformational ensemble from underdetermined macromolecular structural data. *J. Am. Chem. Soc.* **135**, 16595–16609 (2013).

40. Jeschke, G. Protein ensemble modeling and analysis with MMMx. *Protein Sci.* **33**, e4906 (2024).

41. Lyle, N., Das, R. K. & Pappu, R. V. A quantitative measure for protein conformational heterogeneity. *J. Chem. Phys.* **139**, 121907 (2013).

42. Lazar, T. *et al.* Distance-Based Metrics for Comparing Conformational Ensembles of Intrinsically Disordered Proteins. *Biophys. J.* **118**, 2952–2965 (2020).

43. Aina, A., Hsueh, S. C. C. & Plotkin, S. S. PROTHON: A Local Order Parameter-Based Method for Efficient Comparison of Protein Ensembles. *J. Chem. Inf. Model.* **63**, 3453–3461 (2023).

44. Lindorff-Larsen, K. & Ferkinghoff-Borg, J. Similarity measures for protein ensembles. *PloS One* **4**, e4203 (2009).

45. González-Delgado, J. *et al.* WASCO: A Wasserstein-based Statistical Tool to Compare Conformational Ensembles of Intrinsically Disordered Proteins. *J. Mol. Biol.* **435**, 168053 (2023).

46. Scalvini, B. *et al.* Circuit Topology Approach for the Comparative Analysis of Intrinsically Disordered Proteins. *J. Chem. Inf. Model.* **63**, 2586–2602 (2023).

47. Lotthammer, J. M. & Holehouse, A. S. Disentangling Folding from Energetic Traps in Simulations of Disordered Proteins. *J. Chem. Inf. Model.* **65**, 2897–2910 (2025).

48. Cavender, C. E. *et al.* Structure-Based Experimental Datasets for Benchmarking Protein Simulation Force Fields. Preprint at https://doi.org/10.48550/arXiv.2303.11056 (2025).

49. Hellenkamp, B. *et al.* Precision and accuracy of single-molecule FRET measurements—a multi-laboratory benchmark study. *Nat. Methods* **15**, 669–676 (2018).

50. Nüesch, M., Ivanović, M. T., Nettels, D., Best, R. B. & Schuler, B. Accuracy of distance distributions and dynamics from single-molecule FRET. *Biophys. J.* (2025).

51. Montepietra, D. *et al.* FRETpredict: a Python package for FRET efficiency predictions using rotamer libraries. *Commun. Biol.* **7**, 298 (2024).

52. Trewhella, J. *et al.* A round-robin approach provides a detailed assessment of

biomolecular small-angle scattering data reproducibility and yields consensus curves for benchmarking. *Acta Crystallogr. Sect. Struct. Biol.* **78**, 1315–1336 (2022).